Nano Today 26 (2019) 176–198

Contents lists available at ScienceDirect

Nano Today

journal homepage: www.elsevier.com/locate/nanotoday

Review

# Programmable three-dimensional advanced materials based on nanostructures as building blocks for flexible sensors

Zheng Lou[a,1], Lili Wang[b,1], Kai Jiang[c], Guozhen Shen[a,d,*]

[a] State Key Laboratory for Superlattices and Microstructures, Institute of Semiconductors, Chinese Academy of Sciences, Beijing 100083, China
[b] State Key Laboratory on Integrated Optoelectronics, College of Electronic Science and Engineering, Jilin University, Changchun 130012, PR China
[c] Institute & Hospital of Hepatobiliary Surgery, Key Laboratory of Digital Hepatobiliary Surgery of Chinese PLA, Chinese PLA Medical School, Chinese PLA General Hospital, Beijing 100853, China
[d] Center of Materials Science and Optoelectronic Engineering, University of Chinese Academy of Sciences, Beijing 100029, China

ARTICLE INFO

*Article history:*
Received 16 January 2019
Received in revised form 26 February 2019
Accepted 18 March 2019
Available online 31 March 2019

*Keywords:*
Multilevel structure
3D micro- and nanostructures
Structurally engineered behaviors
High performance
Flexible sensors

ABSTRACT

Flexible sensors have garnered a substantial amount of attention recently owing to their potential to revolutionize human lives. The core issue of the growth of high-performance flexible sensors is controlling the attributes of material systems. For the purpose of realizing exotic functions, the use of efficient and extremely practical three-dimensional (3D) systems in device structures is termed as an attractive solution because complex 3D structures are capable of achieving customized behaviors with not only optical but also thermal, mechanical and electrical attributes, which extend their degrees of practicality beyond those that can be attained with conventional, planar material systems. In this review, we first discuss methodologies for the fabrication of 3D multilevel architectures and explain how these programmable materials are capable of enhancing the performance of flexible sensors. Because the electrical, optical and mechanical properties of programmable materials are affected by their structure, shape and size, these factors are of crucial significance in the design and function of flexible sensors. Finally, we offer a discussion on not only recently developed structural materials and their potential applications in flexible sensors but also the key challenges and future directions of this field.



**Contents**



* Corresponding author.
*E-mail address:* gzshen@semi.ac.cn (G. Shen).
[1] These authors contributed equally to this work.

https://doi.org/10.1016/j.nantod.2019.03.002
1748-0132/

## Introduction

Flexible sensors are inevitable components of next-generation flexible electronics, and they have emerged as a fascinating and popular topic in both science and business fields because of their capability to bring forth yet another revolution in the human way of life [1–7]. Efforts to produce state-of-the-art flexible sensors that are sufficiently robust and durable to withstand mechanical damage have resulted in reports of high-performance electronic materials [1]. Nevertheless, the majority of commercial substances with reasonable electronic characteristics are prone to exhaustion, and show poor sustainability when subjected to large deformations, making it quite difficult to directly integrate them into the development of flexible and stretchable devices. Thus, the key aims deal with establishing methodologies for controlling the characteristics of material systems and the features of resulting developed devices, not just through chemistry and morphology but also through three-dimensional (3D) architectures.

In addition, the growth of strategies to form 3D programmable structures in advanced materials is gaining increasing attention due to the capacity to create material systems that basically have different characteristics and functions [8–13]. Some of these 3D programmable structures can display different physicochemical characteristics much different from those of current materials. For example, metamaterials, or cautiously structured materials, usually comprise sporadically arranged building blocks, which manifest characteristics and functions differing from and surpassing those of their constituent materials instead of simply bringing them together [14]. A number of these types of 3D structure designs are derived from advanced assembly technologies (e.g. printing processes, folding processes, and lithography techniques.), in part owing to the different kinds of intricate structures that can be attained by manipulating nanomaterials that have predefined patterns [15]. Recent research has establishded systematic rules for 3D printing techniques for the achievement of micro/nanoscale architectures. Lewis et al. demonstrated an omnidirectional printing method for the fabrication of patterned silver microelectrodes [16]. The patterned microelectrodes are capable of withstanding recurring bending and stretching to large strains with little electrical characteristic degradation. In addition to 3D printing techniques described previously, ideas based on the principles of origami and kirigami together with mechanical assembly have complementary potential to provide major benefits as they are compatible with contemporary planar technologies and linked thin-film accumulation and processing methods [17,18]. Furthermore, lithography techniques make use of 3D structures developed through the use of light to offer considerable flexibility in geometric designs [15]. For this reason, these 3D structures are typically used as building blocks to provide a new avenue for the creation of new structural and functional materials.

3D programmable structures in advanced materials typically display outstanding optical, thermal, electrical, and mechanical properties, which suggest superior advantages in flexible sensor applications (Fig. 1). Advancements in these applications depend on developments in materials and methods for fabricating 3D structures. For instance, 3D programmable architecture materials exhibit robust deformable systems benefiting from their disparate 3D or 2D features by means of printing, loading and lithography technologies, thereby providing a desirable means of integrating different kinds of ideal mechanical behaviors, including linear deformability (i.e., compressibility and stretchability), flexibility, twistability and bendability [20,21]. Therefore, in constructing flexible sensors, architectural design on the nano- and microscales stemming from the growth of nanotechnology can serve as a strategy for rendering rigid electronic materials capable of accommodating the macromechanical strain that prevails in intricate settings. Lightweight materials with high moduli can also be attained with cautiously designed 3D periodic units that contain elements accommodating mechanical deformation to realize flexible and stretchable sensors while maintaining their electronic behavior [2]. Furthermore, mimicking 3D structure-based mechanisms for fabricating flexible sensors with specific functionalities can enhance the fundamental efficiency of such devices and lead to new concepts for flexible sensor applications. In addition to the above applications, 3D programmable structures also have promise for use in different types of growing fields, e.g., energy storage [22,23], robotics [24], and catalysis [25]. Although several reviews have briefly discussed aspects of the use of 3D structures [26–28], until now, there have been no comprehensive reviews focusing on 3D programmable structure-based flexible sensors.

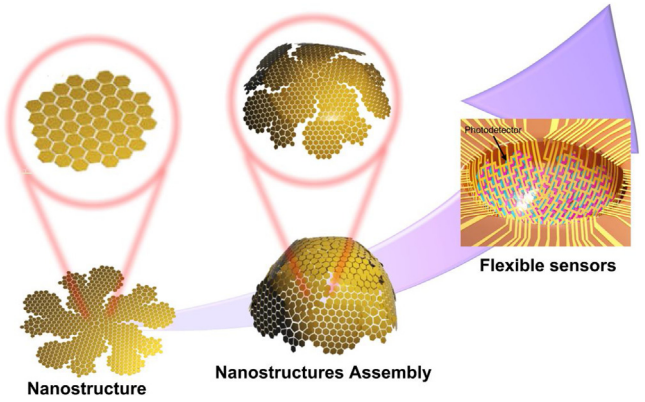


**Fig. 1.** An overview of this review highlighting programmable 3D nanostrcuture materials-based flexible sensor, including nanostrucure assembly techniques, advantage using these programmable 3D nanostrcuture and their flexible sensors application. Reproduced with permission [19]. Copyright 2017 Nature Publishing Group.

The current review sheds light on recent findings involving the use of 3D programmable structures in advanced functional materials for flexible sensors. The first section discusses various techniques (e.g., printing, folding, and lithography) for fabricating 3D micro/nanostructures. Subsequent sections summarize structurally engineered behaviors in properties of interest, including optical, electrical and mechanical properties, of flexible sensors, e.g., strain and pressure sensors, photodetectors biosensors, and gas sensors. The conclusion outlines some challenges and opportunities for the prospective investigation of advanced 3D programmable structures.

## Design strategies for the assembly of 3D micro/nanostructures

### *Printing processes*

Printing, which is an effective and reproducible method, can be used to build 3D structures on various substrates with a tuned shape and size for various applications, especially the fabrication of large-area flexible sensors [29]. 3D printing provides exceptional mechanism flexibility, coupled with geometric controllability. In addition, printing has the ability to attain extensively elevated throughput using low raw material usage, allowing substantially reduced costs [30]. Several printing technologies are used to manufacture flexible sensors, including gravure printing, screen printing, transfer printing and inkjet printing [31]. The most extensively employed method for 3D printing is dependent on externally controlling the scanning deposition nozzles wherein 1-3D structures are developed in a layer-by-layer manner. Materials usually developed for particulate and/or polymeric species having the intended rheological properties play the role of 'inks'. According to the characteristics of ink and the nature of the transport process, these technologies can be further divided into two categories: liquid ink jet printing and micro-extraction printing of viscoelastic ink [32–34]. These versatile methods can facilitate the assembly of extremely oriented and patterned micro/nanowire/fiber arrays on various substrates with control over the layers, density and pitch. Very sophisticated 3D architecture materials can be easily achieved by means of 3D printing (Fig. 2) [35,36], with intricacy in the planar and/or 3D spaces.

Traditional, convenient methods have been developed through the use of various 3D printing techniques. Specific space architectures with sporadic or aligned pores allow rapid ion transport, which is beneficial for rapid charging/discharging; in addition, the augmentation of substances by loading in the third dimension is expected to immensely amplify their sensing capability. Recent studies have established methods for the fabrication of complex 3D structures at a micro/nanoscale resolution in an extensive array of substances, including inks based on concentrated nanoparticles (NPs) [37,38], polymers [39,40], colloids [41–43], and carbon materials [44,45]. In addition, the primary regions of prevailing interest are in conductive inks due to their significance in major applications, from rigid to flexible and wearable sensors. The following subsections shed light on some of the recent advancements that have been made.

*1D nanowire assemblies by inkjet printing.* Inkjet printing involves the use of nozzles via thermal or electrical mechanisms for the purpose of delivering liquid drops to intended areas on a substrate and has been recently used for the assembly of nanowires/fibers [46,47]. The printability of inks is primarily determined by three important parameters of fluids, i.e., the surface tension, density, and viscosity. A suitable viscosity, density and surface tension are essential for producing droplets without clogging the nozzles. Coleman et al. reported the production of semitransparent silver nanowire arrays with good optical conductivity ratios of ~40 fabricated by inkjet printing (Fig. 3a-d) [48]. In addition, it is quite convenient to control lateral characteristics, for instance, the length and width of printed lines. Ag nanomaterials dispersed in isopropyl alcohol alone cannot effectively be made into nanowires by inkjet printing; due to the low viscosity and the consequent development of satellite drops, the ink disperses during flight from the printing head to the substrate. However, an optimized suspension with a suitable viscosity ($\eta = 4.6 \pm 0.3$ mPa s) and surface tension ($\gamma = 28$ mJ/m$^2$) can be printed precisely on fixed areas to create high-aspect-ratio features with no satellite drops. In addition to this investigation, Lewis et al. incorporated changes into the ink composition through the introduction of stable, particle-free silver precursor inks (Fig. 3e) [16]. After this printing step, a gel-based 1D silver line (5 μm wide) was printed on a silicon substrate (Fig. 3f). In this work, silver acetate was dispersed in ammonium hydroxide for the purpose of making an aqueous ink. The reactive silver ink could be directly printed on the substrate for the production of 1D-structures with high transparency and high electrical conductivity, thereby opening new avenues for the integration of printed sensors.

*2D/3D nanowire assembly inkjet printing.* Microextrusion printing offers more opportunities for 3D structuring because of the extensive array of ink designs and feature sizes. A printing head robotically controls the extrusion of an ink onto a substrate, wherein a handling and dispensing system pneumatically or mechanically (using a piston or screw) controls the extrusion of a substance in fully-defined ambient environment. Wang et al. proposed a retrofitted inkjet printing process for the controlled mass production of high-quality microwire arrays (Fig. 4a) [49]. This technique uses a syringe as a printing head, coupled with two slits with contrasting forces, controlling the self-assembly of micro/nanowires. Through movement of the platform, the protruding microwire ends are primarily attached to a flexible substrate; subsequently, the rest of the length and direction is determined using a computer program to control movement on the x and y- axes. $Zn_2GeO_4$ microfibers can be 3D-printed in a direct manner on a flexible polyimide (PI) substrate for the formation of an aligned wire array. By changing the direction of the movement of the printing head on the x- and y- axes, convenient control over the formation of nanowires is possible (Fig. 4b-f). This technique is likely to be helpful in the development of more complex methods, capable of fabricating intricate computer circuits.

Fig. 4g–l presents information on the use of inorganic materials (ZnO (Fig. 4g, j) [50,53], $In_2O_3$ [54],) organic materials (polylactic acid, Fig. 4h,k) [51] and biomaterials (chitosan, Fig. 4i, l) [52] to print micro/nanofiber arrays. Each method can produce patterns with outstanding uniformity and without errant droplets, which confirms the exceptional dependability and efficacy of these methods. In addition, the micro/nanowires/fibers are unchanged after calcination to remove impurities, as presented by the optical micrographs and SEM images, respectively (Fig. 4g–l).

Mechanical printing has been used for the fabrication of 3D multinanowire structures. Printable graphene oxide (GO) gel inks have been printed to stack 3D structures at room temperature in a direct manner (Fig. 5a–c) [55]. Low concentrations of GO ink with cCa $\approx 15 \times 10^{-3}$ m have been used as gel inks. The GO gel ink is loaded into a movable syringe, controlled by a programmable robot deposition arm and extruded through a nozzle to deposit 3D structures with good homogeneity and optimum elasticity ($G' \approx 10^4$ Pa). Recently, Zhu et al. reported an innovative, novel aqueous GO ink and demonstrated the fabrication of graphene aerogel microlattices printed using the developed ink (Fig. 5d) [56]. They additionally used the graphene-based composite aerogels to assemble a sandwiched supercapacitor. Through the logical design of the electrode structure, the 3D printed graphene structure shows the potential of high quality loading and structure customization to improve power density.

### *Folding processes*

The pervasive presence of effective and extremely functional 3D systems in biology indicates that the same types of architectural designs could be beneficial in flexible sensor applications by extending the degree of functionality beyond what can be attained using conventional, planar 2D platforms [12]. There are several examples of the worth of 3D structures in achieving unique characteristics using straightforward substances (Fig. 6) [19,20,57–59]. In addition, advancements in this area are usually constrained by the

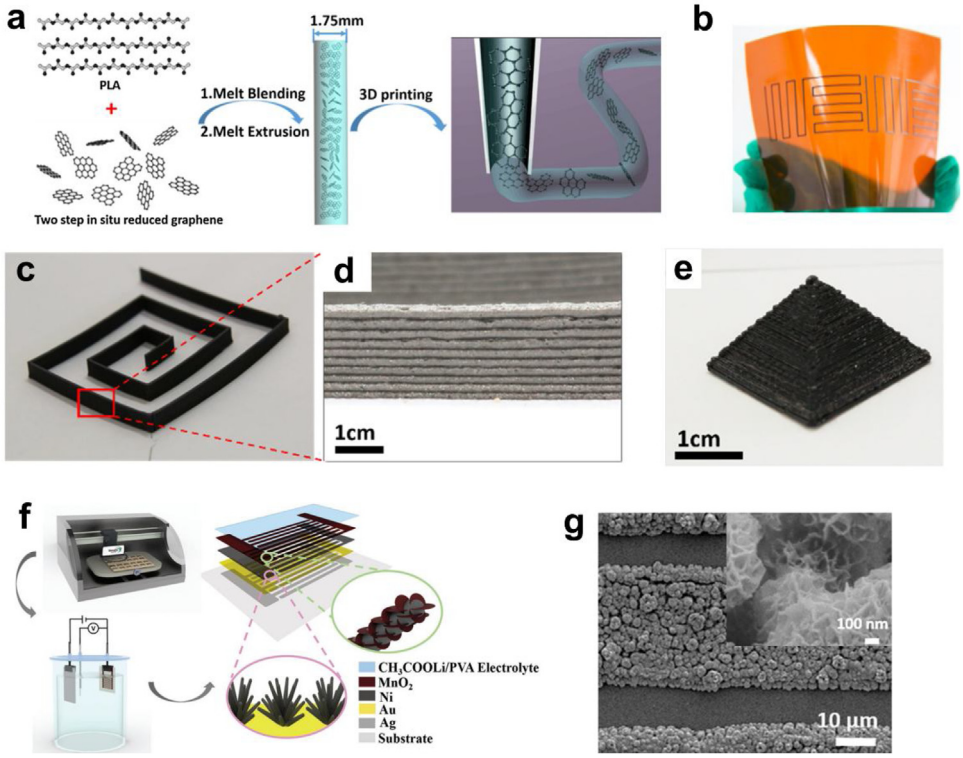


**Fig. 2.** (a) The simplified schematics of the FDM 3D printing process based on graphene. (b) Flexible circuits pattern based on PI substrates. (c) 3D printed flexible circuits, (d) enlarged drawing of the selected part of (c). (e) Mini pyramid based on 3D printed. Reproduced with permission [35]. Copyright 2016 Elsevier B.V. (f) Schematic illustration of the printable fabrication procedure. (g) SEM images of 3D nanocoral-structured electrodes. Reproduced with permission [36]. Copyright 2017 WILEY-VCH Verlag GmbH & Co. KGaA.

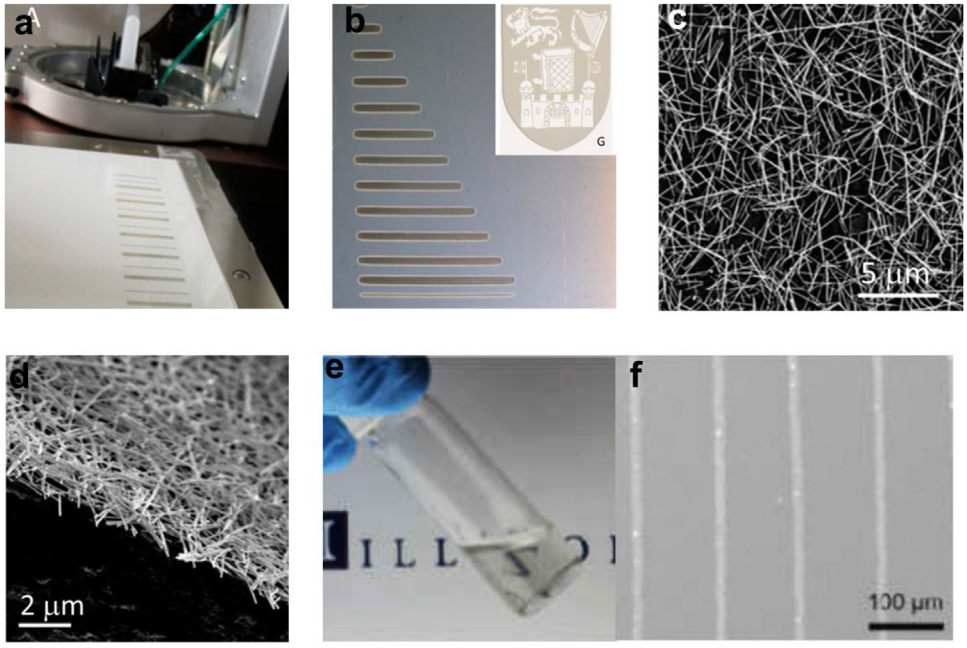


**Fig. 3.** (a) Ag NW networks fabricated by Inkjet-printing method. (b) Inkjet printing of Ag NW lines on PET substrate with array strcuture. (c) Top view and (d) cross-section view SEM images of silver nanowire networks. Reproduced with permission [48].Copyright 2015 American Chemical Society.(e) Optical image of silver ink in a scintillation vial. (f) Printed silver wire array on the surface of Si substrate by using 3D printing method. Reproduced with permission [16].Copyright 2015 American Chemical Society.

relatively smaller range of options in not only controlled but also dependable and reproducible strategies for the production of 3D geometrical shapes using state-of-the-art functional substances. One of the most recently proposed methodologies is a scheme wherein the detailed buckling linked to a stretched elastomeric substrate provides guidance for the mechanical assembly of intricate 3D structures, some with designs similar to those that can be achieved at the macroscale by means of origami/kirigami [60,61]; these structures can having particular shapes and sizes and are capable of spanning numbers of orders of the magnitude in prop-

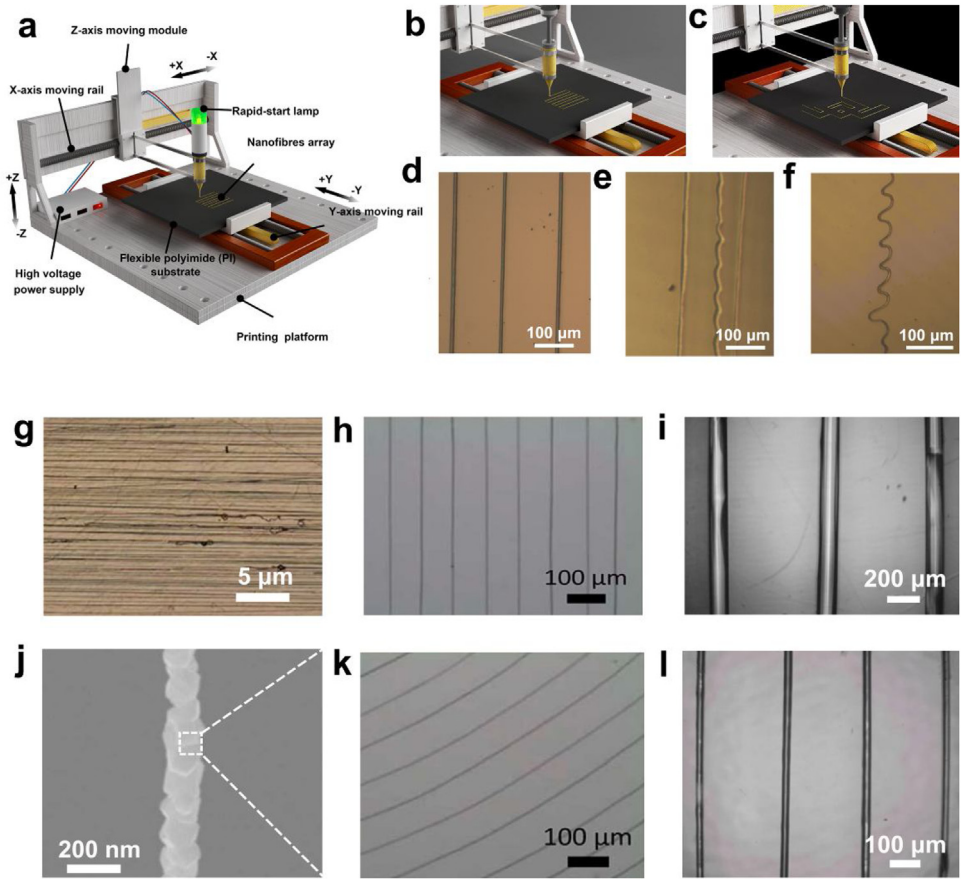


**Fig. 4.** (a) Schematic diagram of printing setup for fabricating $Zn_2GeO_4$ wire. (b–c) Schematic diagram of printing setup of various morphologies of printed fibers. Optiocal images of various shapes of printed fibers: (c) nanowire array; (e) aligned and wavy fiber, and (f) wavy fiber. Reproduced with permission [37]. Copyright 2018 WILEY-VCH Verlag GmbH & Co. KGaA. (g) Optical and (j) SEM images of printed ZnO nanofiber arrays. Reproduced with permission [50]. Copyright 2014 Nature Publishing Group. (h–k) Optical images of printed polylactic acid wire arrays. Reproduced with permission [51]. Copyright 2016 IOP Publishing. (i, l) SEM images of printed chitosan wire arrays with different shape. Reproduced with permission [52]. Copyright 2013 Springer.

erty aspects, down to the submicron scale in the lateral functions, while being tens of nanometers thick [62].

Origami, from 'ori,' which means folding, and 'kami' which means paper, is an indication of the old Japanese art of paper folding [24]. Folding gives rise to an extensive array of intricate morpho-functional structures naturally, such as with, proteins and intestines, in addition to enabling the growth of structures, such as with flowers, leaves and insect wings [63]. For intricate 3D structures inspired by origami, folding has promise as a route for 2D to 3D alterations [64]. Starting with an individual sheet of paper or even a linear string, intricate 3D objects that have unique mechanical characteristics can be developed via folding [65]. Thus, ideas derived from the ancient art of origami and from nature are applicable for the creation of a novel category of effective and extremely functional 3D substances. This section focuses on the folding methods caused by internal stress, including the two most advanced methods based on 4D printing, as well as micro and nano origami [34].

4D printing follows traditional 3D printing with a shape-morphing step and can be used to make more intricate shapes than those feasibly achieved by traditional 3D printing [66]. One example of ceramic-based 4D printing is the use of elastomeric polydimethylsiloxane matrix nanocomposites in programmable architectures [67], wherein the hierarchical matrix exhibits remarkable properties of conventional ceramics, such as high thermal stability, mechanical resistance to tribology and chemical resistance to oxidation and corrosion (Fig. 7a–f). Another impressive example is reversible shape changing structures that can be achieved by grayscale pattern 4D printing [68]. Various self-folding structures were printed via desolvation stimulated by bending deformation (Fig. 7e–g). When the bent structure is placed into solution with the appropriate solubility parameters, in addition to reduced crosslinking, this material can absorb solutions (such as acetone) and expand, forcing the bending structure to recover. Because PEGDA with lower crosslinking degree has reasonable swelling potential in acetone, acetone can cause swelling, and the swelling feedback is fast due to the same swelling parameters. The acetone molecules are expected to diffuse out of the structure, allowing the structure to bend once again (Fig. 7f) and reversing the shape change. Accordingly, 4D printing is a straightforward and economical means of creating active structures with great potential for applications with composite substances, such as soft robotics and endovascular stents.

*Micro/nanoscale origami.* Folding deformation has the potential to serve as the underlying foundation for origami-inspired assembly at the micro/ nanoscale [70,71]. In the majority of published reports, rigid nanocomposite sheets can attain atypically elevated extension after fabrication by microscale kirigami patterning, which is the result of stress delocalization over a number of deformation points. Folding methodologies are capable of not only paving the road for the use of predictive deformation mechanics in such intricate substances as composites but also allowing the systematic engineering of elasticity. In conventional kirigami, a pattern of cuts is made in paper sheets, to attain the targeted topology upon folding. Recently, Zhu et al. developed a new approach for the shape morphing of 2D composite sheets, which was guided

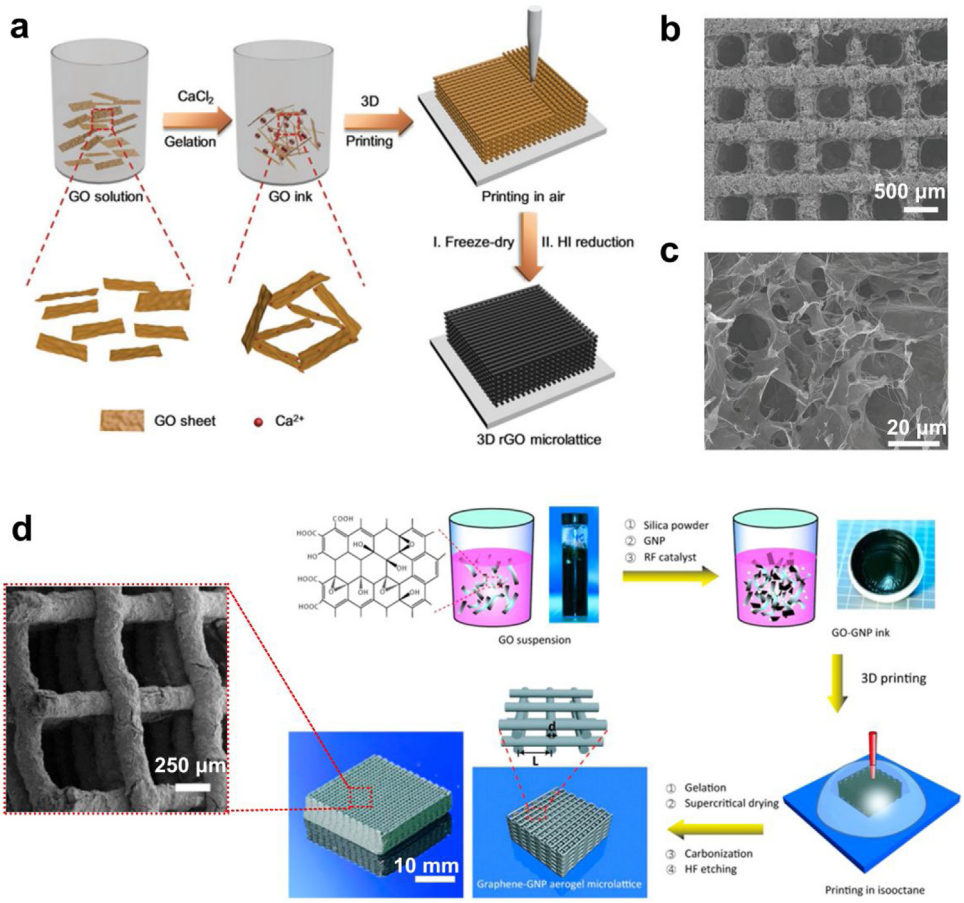


**Fig. 5.** (a) Schematic illustration of 3D printing process of rGO aerogel microlattices. (b) SEM images of 3D rGO nanosheet-based aerogel microlattic. (c) SEM image of rGO nanosheets. Reproduced with permission [55]. Copyright 2018 WILEY-VCH Verlag GmbH & Co. KGaA. (d) Schematic illustration of 3D printing process of graphene nanoplatelets. Inset show the SEM image of graphene nanoplatelets-based aerogel microlattic. Reproduced with permission [56]. Copyright 2016 American Chemical Society.

by origami/kirigami design rules, followed by stimulation by a laterally nonuniform strain (Fig. 8a–b) [60]. The composite sheet underwent laterally nonuniform shrinkage upon heating, changing the Gaussian cur-vature of the sheet and transforming the flat sheet into a curved 3D structure. Other examples of folding-based programmable structures make use of GO as nanoscale building blocks for the fabrication of all-graphene self-folding paper, wherein the self-folding material responds to light and exhibits swelling characteristics (Fig. 8c) [69]. By means of the rational design of programmable architectures, integrated GO-PDA/rGO paper could achieve high mechanical strength and stability. The GO-PDA layer is capable of absorbing water from the atmosphere, which leads to swelling, while water is lost upon NIR/laser light irradiation, stimulating shrinkage (Fig. 8d).

*Lithography-based 3D writing technologies*

Lithography-based 3D writing technology is considered the most widespread micro/nanoscale patterning methodology due to its productivity and performance [75]. The term photolithography carries a literal translation of writing in stone with the use of light based on the Greek origins of the term. Usually, the “stone” is a silicon wafer layered with a light-sensitive polymer. The exposure of this polymer to light (or electrons/ions) modifies the solubility of the polymer in local areas of a given pattern; the mechanism is demonstrated in Fig. 9a [72]. Contrary to nozzle-based methodologies, these approaches are effective applied using a thin array of substances while still offering outstandingly resolution and printing speeds. Murray et al. reported planar arrays based on $VO_2$ nanopillars and nanowires fabricated by nanoimprint lithography (Fig. 9b) [73]. They first prepared colloidal metallic $VO_2$ nanocrystals (NCs), followed by patterning a nanostructured Si master as a structure template (size and shape) on the surface of polymer resist by nanoimprint lithography. Then, a thin layer of colloidal NCs is spin-coated on the topmost surface of the patterned substrate, and the polymer resist is then lift-off for the deposition of patterned $VO_x$ thin films. In addition, phase-changing $VO_2$ nanostructures can be produced through the use of rapid thermal annealing. In the current work, nanopillars and nanowires with diameter of 300 nm and 100 nm were attained (Fig. 9c–d). Moreover, the pattern of the 3D structures was controlled by the light exposure patterns.

Yang et al. combined a centrifugation methodology with conventional photolithography for the fabrication of 1D arrays on the basis of GO nanosheets and $SiO_2$ nanoparticles (Fig. 9e) [74]. They first prepared gold electrodes, followed by patterning with the photoresist (AZ 5214) on a silicon oxide substrate via photolithography and lift-off. The bottom of the silicon oxide wafer was then functionalized with a thin layer of 3-aminopropyltriethoxysilane (APTES), which has a positive charge, as well as a cysteamine composite, coupled with the gold facade (Fig. 9f). Subsequently, negatively charged GO-NPs were immobilized on the patterned photoresist substrate surface (electrostatic interactions) via centrifugation. A high density and uniform GO-$SiO_2$ NP array was attained through the removal of the patterned photoresist with the use of acetone (Fig. 9g). This work provides a methodology for the fabrication of devices with wire array structures and the affordable production of related devices at an extensive scale via photolithography.

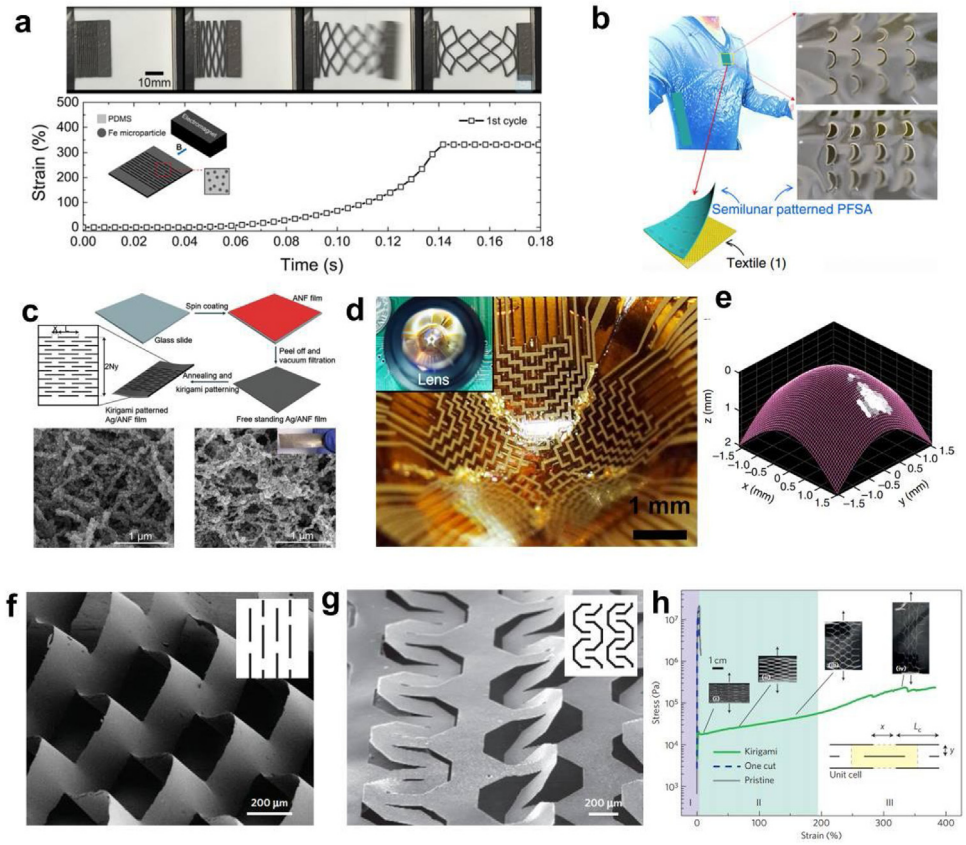


**Fig. 6.** Optical images and strain response curve of Fe-PDMS materials with 3D kirigami structure in response to an external force (magnetic field). Reproduced with permission [57]. Copyright 2018 Nature Publishing Group. (b) Flexible humidity and thermal sensor based on a perfluorosulfonic acid ionomer film with semilunar patterns. Reproduced with permission [58]. Copyright 2018 Nature Publishing Group. (c) Schematic illustration of the kirigami pattern process and SEM images of ANF films. Reproduced with permission [59]. Copyright 2017 AIP Publishing. (d) Optical image of the hemispherical focal plane arrays based on origami silicon optoelectronic devices. Inset image exhibits the optical image of the electronic focal plane array-based on eye system. (e) Hemispherical origami silicon-based electronic eye camera shows the laser point. Reproduced with permission [19]. Copyright 2017 Nature Publishing Group. (f–g) SEM image of GO-PVA nanocomposites with different kirigami patterns. (h) Stress–strain curves for GO-PVA kirigami sheet under different tensile states. Reproduced with permission [20]. Copyright 2015 Nature Publishing Group.

## Advantages of multilevel architecture materials for flexible sensors

Structural design is a robust methodology for producing flexible sensors as it allows improvements in the stretchability of substances ranging from soft to stiff [76]. With regard to the past two decades, complex 3D structures with tunable optical, thermal and electrical fields and highly unusual attributes have been reported; for instance, highly deformable properties, excellent transport properties, high-aspect ratio features and high photoabsorption have been demonstrated (Table 1).

With regard to optical properties, a logical design, coupled with the self-assembly of photonic nanoarchitectures with fully defined structures and geometries, allows for the precise manipulation of light at the nanoscale, which has been a key emphasis of flexible photosensors in recent decades. Ma et. al. proposed a straightforward origami methodology for fabricating monocrystalline silicon-based focal plane arrays and compound eyes with hemispherical structure (Fig. 10a–d) [19]. Using each polygon block as sensor pixel, silicon-based devices are fabricated into short icosahedral networks and artificial flexible plate networks, and further folded into concave or convex hemispheres (Fig. 10e-f). On the basis of the concave or convex hemisphere, camera system applications have been illustrated, e.g., high-resolution hemispherical electronic lenses that have a larger field of view, improved atypical imaging, and enhanced performance compared with planar devices (Fig. 10g–h).

With regard to mechanical attributes, kirigami designs allow sheets to reach a level of stretchability approximately 2 times greater in magnitude than that of pristine sheets (from 2% to 750%) [57]. As evident from Fig. 11, adding small cuts substantially alters the deformation behavior of a kirigami film, which results in reduced rigidness and greater elongation compared with a kirigami film that comprises only key cuts. Being specific, while hanging weights, a kirigami system comprising merely key cuts reveals non-significant strain ($\varepsilon \approx 0\%$) until the force reaches 0.4 N. In contrast, a modified system with large and small incisions begins to extend under much lower force (0.1 N) and achieves more than 270% strain at 0.4 N. The smaller cuts also augment the eventual extensibility of films, as shown in Fig. 11b.

With regard to electrical characteristics, integration of the intended mechanical and electrical attributes at the fiber level is considered the most efficient but is still an uncommon strategy concerning flexible sensor applications. It is possible to fabricate stretchable conductive fibers by means of wrapping conductive substances (e.g., carbon nanotubes (CNTs) and graphene) around elastic fibers (e.g., poly(styrene-block-butadiene-block-styrene) and polyurethane). Conductive substances have the potential to offer electrical conductivity, tensile strength, mechanical and thermal stability. For instance, aligned multiwall CNT sheets developed via chemical vapor deposition can be narrowly wound onto an elastic rubber fiber at a precisely designed helical angle, which results in a fiber that has a stretchability amounting to 100%, in addition to a maximum resistivity of 0.086 kΩ $cm^{-1}$ (Fig. 12) [92].

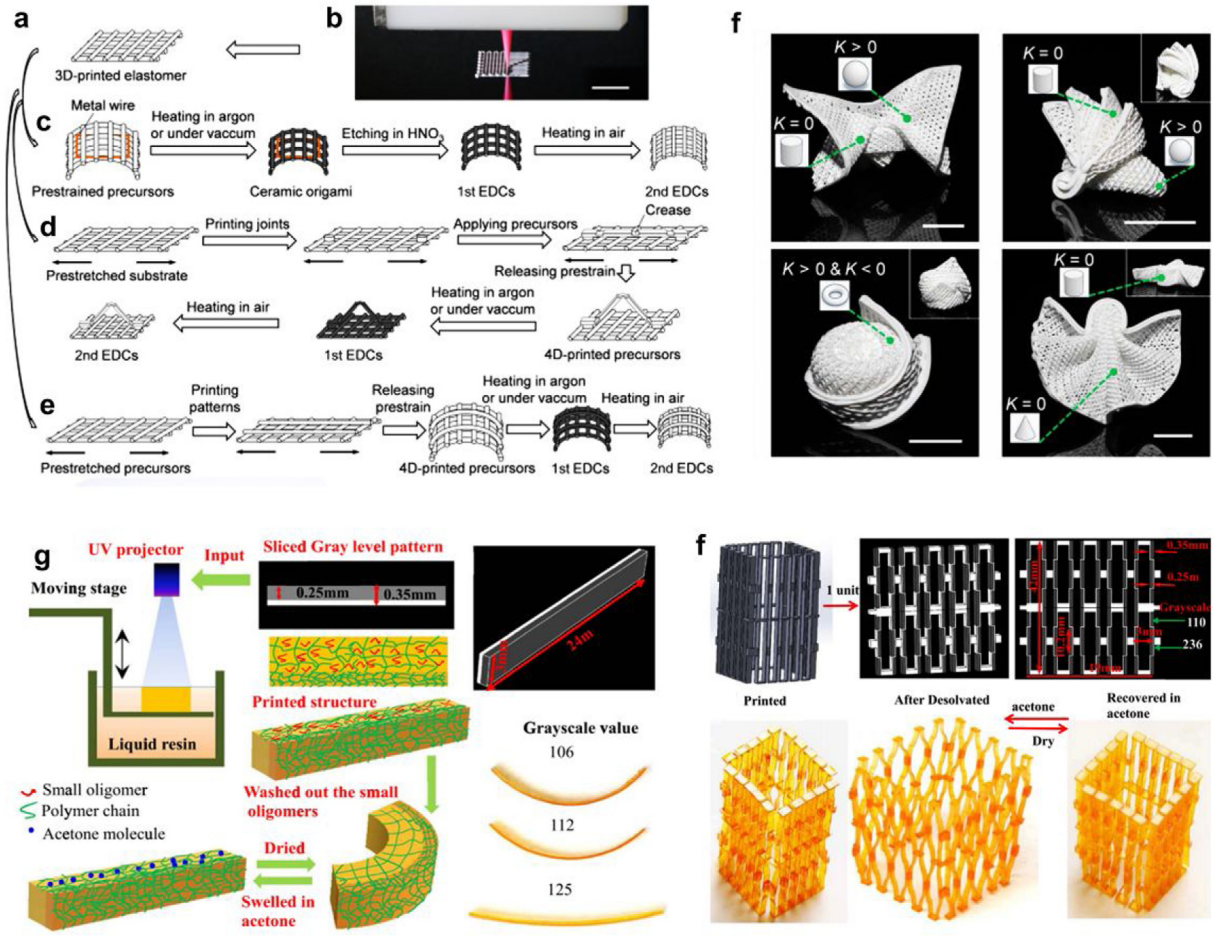


**Fig. 7.** (a–e) Printed 3D elastomeric lattices was obtain by using 4D printing method. (f) Ceramic origami structure with different K (spherical caps). Reproduced with permission [67]. Copyright 2018 Science. (g) Schematics to show the grayscale 4D printing progress. (h) 3D self-expansion/shrinkage structure with acetone and air conditions. Reproduced with permission [68]. Copyright 2018 IOP Publishing.

**Table 1**
Summary of the 3D materials: examples, fabricated method, and advantages.

| Material type | Structure | Method | Advantages | Ref. |
|---|---|---|---|---|
| Holey graphene | Porous mesh architecture | 3D Printing | Mass transport | [77] |
| $\alpha$-$Fe_2O_3$ | Particles-based 3D shapes | 3D Printing | Mechanical robustness | [78] |
| Ni@$MnO_2$ | Hierarchical nano-coral structures | 3D Printing | Flexibility electrochemical stability | [36] |
| $LiFePO_4$ | Multilayer structure | 3D Printing | High-aspect ratio features | [79] |
| Silk fibroin | Interconnected porous structures | 3D Printing | Mechanical suitability | [80] |
| Carbon nanotube | 3D network | 3D Printing | Electrical properties | [81] |
| Graphene | 3D foams | 3D Printing | High conductivity high damping capacity | [15] |
| SiC/C-fiber | Triangular honeycomb arrays | 3D Printing | Mechanical flexibility | [82] |
| Carbon fiber | 3D fiber array | 3D Printing | High sensing and mechanical properties | [83] |
| Cellulose fibrils | 3D fiber alignment | 3D Printing | High sensing and mechanical properties | [84] |
| Cellulose fibrils | 3D flower shape | 3D Printing | High sensing and mechanical properties | [84] |
| Poly(dimeth-ylsiloxane) | Hierarchical structure | 4D Printing/ origami | Good deformation | [67] |
| GO-PVA | Nanosheets-based 3D structure | Kirigami | High elasticity conductivity | [20] |
| CNT | Miura folding | Origami | Excellent mechanical properties | [85] |
| Silicon | 3D hemisphere array | Origami | High photoabsorption flexibility | [19] |
| DNA/Ag | 3D nanoparticles | Origami | Good optical properties | [86] |
| Polyethylene Terephthalate | Sheets-based 3D structure | Kirigami | Excellent mechanical properties | [87] |
| Liquid-crystal | 3D flower | Kirigami | High sensing and high mechanical properties | [88] |
| Graphene paper | 3D structure | Origami | Excellent optical and mechanical properties | [69] |
| Graphene/ $SiO_2$ | Nanosphere based 1D array | Lithography | Excellent transport and sensing properties | [74] |
| Polymer | Multilevel architectures | Lithography | Good mechanical properties | [89] |
| Si | 3D structure | Lithography | Good optical properties | [90] |
| Polymer | 3D structure | Lithography | Good optical properties | [91] |

Several fibers can be wound onto a substrate or knotted into different kinds of shapes. In addition, a stretchable dye-sensitized solar cell that makes use of this fiber as the counter electrode has been reported, reaching a maximum power conversion performance of 7.13% following twenty cycles of stretching at 30% of the tensile strain.

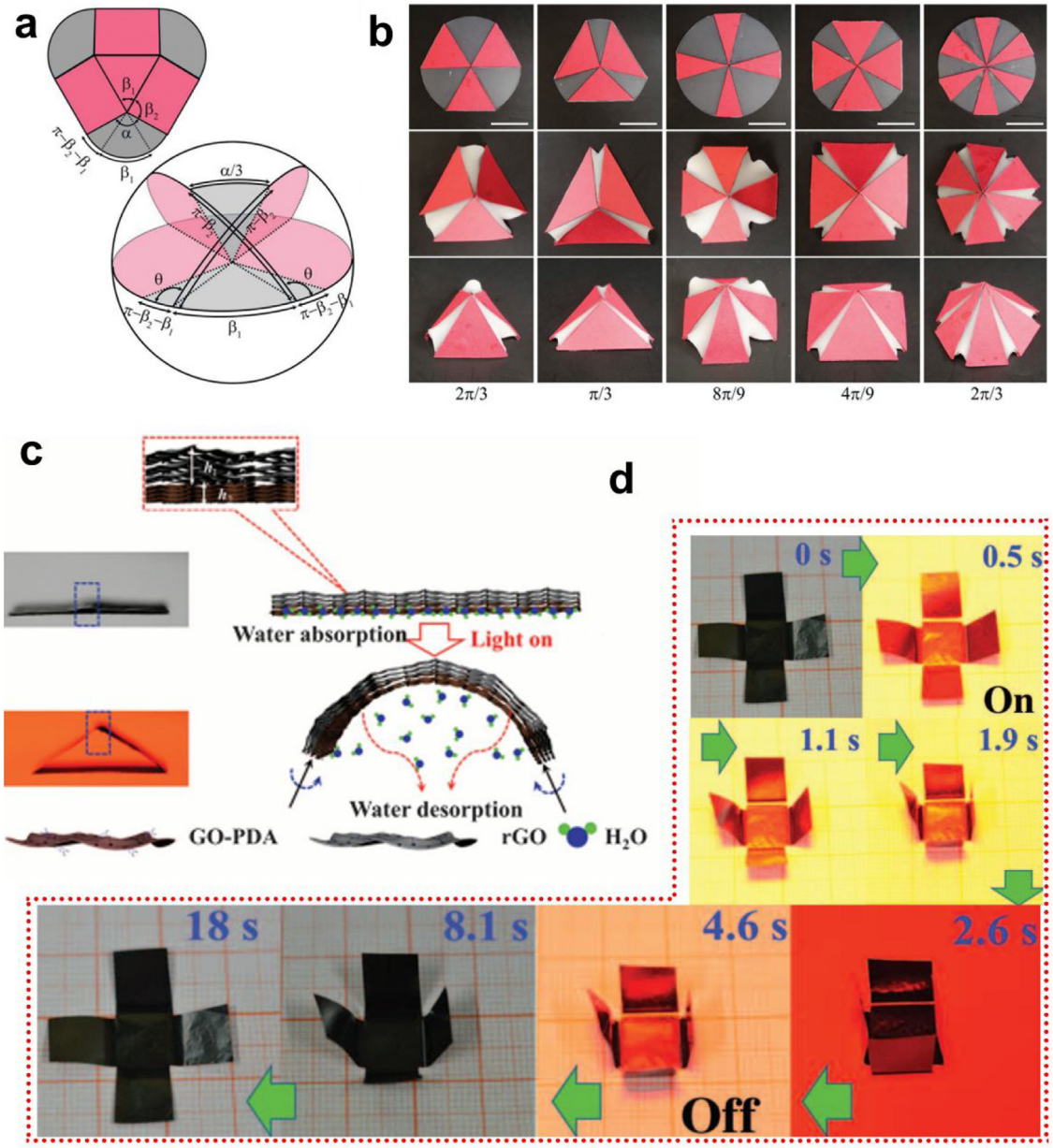


**Fig. 8.** (a) Schematic representation of the folding and related parameters. Red: paperboard sector; blue: PS sector. (b) Folding of cones using multiple angular shrinkage gadgets. Top: before folding; middle: after folding (top view); bottom: after folding (perspective view). Reproduced with permission [60]. Copyright 2018 WILEY-VCH Verlag GmbH & Co. KGaA. (c) Schematic representations of the structures and mechanisms of the graphene paper. (d) A fast self-folding box driven by light with different times. Reproduced with permission [69]. Copyright 2015 AAAS.

## Applications of programmable multilevel architecture materials

### *Flexible mechanical sensors*

As the application of tactile sensors in skin-stimulating electronic devices has gained an increasing amount of attention, electromechanical sensors have been extensively studied [93–96]. There are three main types of electromechanical sensors: pressure, strain and vibration sensors. Each sensing method is based on different materials and properties, which means that each method involves different mechanisms for responding to external mechanical changes. Because programmable 3D microstructures and nanostructured sensing materials can utilize deformation caused by small forces, they show superior performance sensing pressure, mechanical vibration, elongation/compression, bending or torsion and are dominant in this field. Properly arranged fiber arrays usually manifest improved output compared with nonwoven mats or isolated strands. Here, we discuss the fundamental physics involved as well as representative substances with regard to all cases, which are based on the 3D micro/nanostructures in advanced sensing materials.

#### *Pressure sensors*

In particular, flexible pressure sensors have garnered wide appeal owing to their extensive applications in epidermal health examination or motion detection [97–99]. In recent years, researchers have paid extensive attention to the growth of both flexible and stretchable pressure sensors that have high sensitivity to medium pressure [100]. In addition, the sensing mechanisms of these pressure sensors include not only piezoresistive but also capacitance and piezoelectricity [101]. According to the structure

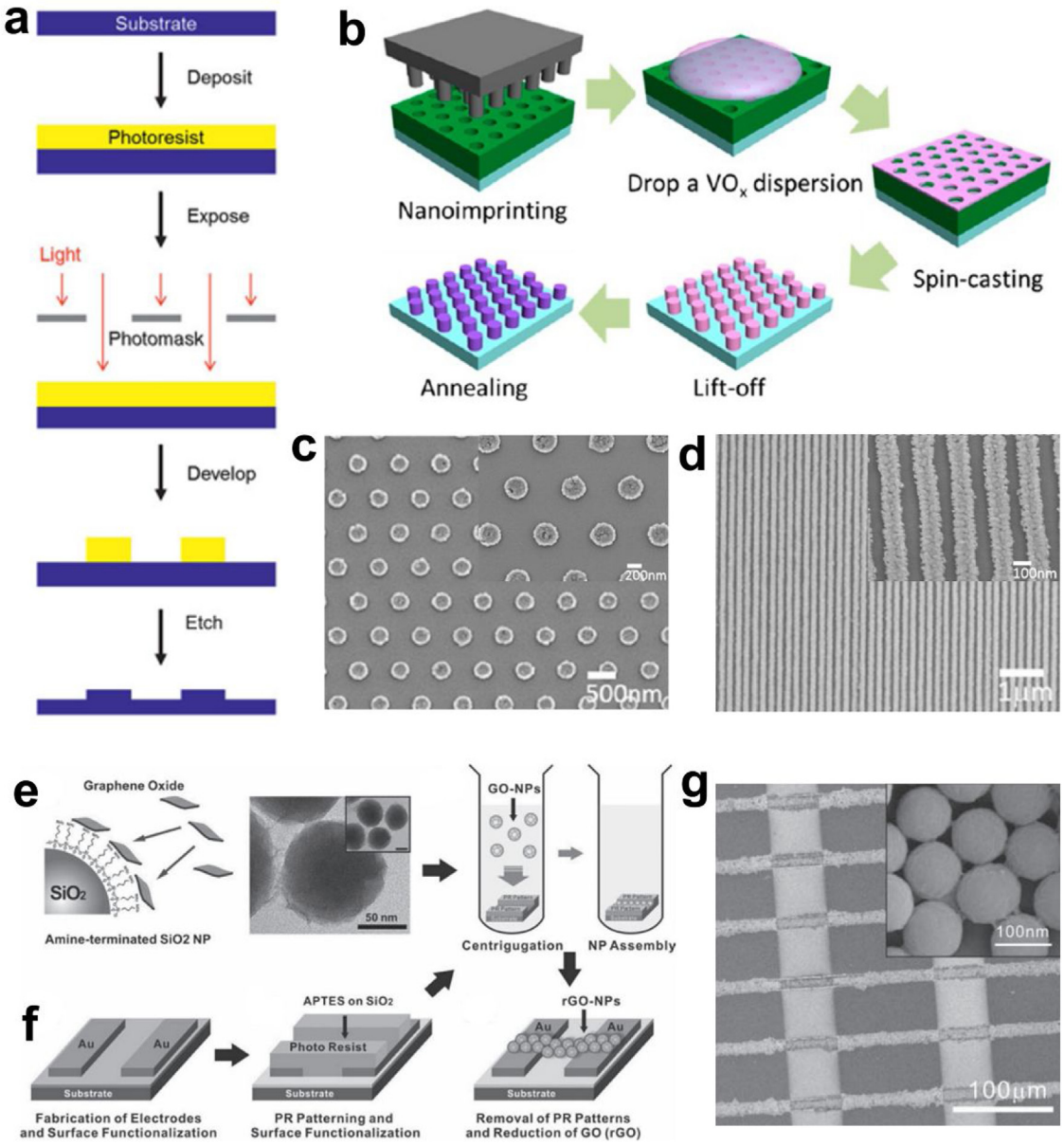


**Fig. 9.** (a) Schematic representation of the conventional photolithography technology. Reproduced with permission [72]. Copyright 2016 Materials Research Society. (b) Schematic of nanoimprint lithography to fabricate subwavelength $VO_2$ nanostructure. SEM images of $VO_2$ nanostructure arrays (c) nanopillars and (d) nanowires. Reproduced with permission [73]. Copyright 2014 American Chemical Society. (e) Schematic diagram of the process of amine-functionalized GO and TEM image of GO-$SiO_2$ nanoparticles (f) Fabrication process of biomolecular sensor based on graphene-coated nanoparticles. Fabrication of a metal electrode. (c) SEM image of GO-$SiO_2$ nanoparticles arrays-based biosensors. Reproduced with permission [74]. Copyright 2011 WILEY-VCH Verlag GmbH & Co. KGaA.

of active substances and devices, all of these sensing processes have their own attributes.

With the use of the basic piezoresistive effect and advanced manufacturing technologies, e.g., contact printing, micromachining and direct writing, a flexible/stretchable pressure sensor can be constructed [102,103]. A contact printing method for the purpose of assembling Ge/Si core/shell NW arrays on PI substrates as active matrix backplanes of flexible pressure sensor arrays ($18 \times 19$ pixels) has been reported by Javey et al. (Fig. 13a-b) [102]. The integrated sensor array can be effectively used as an e-skin to improve the spatial resolution to monitor the applied pressure distribution. Other researchers also demonstrated that such pressure sensor arrays have the potential to be used a printed CNT active matrix TFT backplane for the purpose of plotting the applied pressure on an area [104]. In addition to contact printing, inkjet printing accurately deposits micro/nanomaterials in functional alignment by means of nonimpact, additive patterning and maskless methods, which have attracted great attention in recent years [105]. Furthermore, inkjet printing has been extensively used for manufacturing pressure sensors because of its affordability, variable digital printing patterns and low material consumption [106]. Whitesides et al. produced carbon-based piezoresistive mechanical sensors via inkjet printing on (3,3,4,4,5,5,6,6,7,7,8,8,9,9,10,10-heptafluorodecyl) trichlorosilane (C10 F)-modified paper. The compression resistance of the microelectromechanical system (MEMS) deflection sensor for the inkjet printing decreased throughout the upward deflection [107]. Liu et al. prepared a piezoresistive bending sensor by spraying Ag NWs and double-hydroxide-layered mixed inks on paper substrates with a low permeability threshold. A flexible human motion sensor with nontoxicity, robust bending stability, fast response and recovery times, good sensitivity and low cost was developed [108].

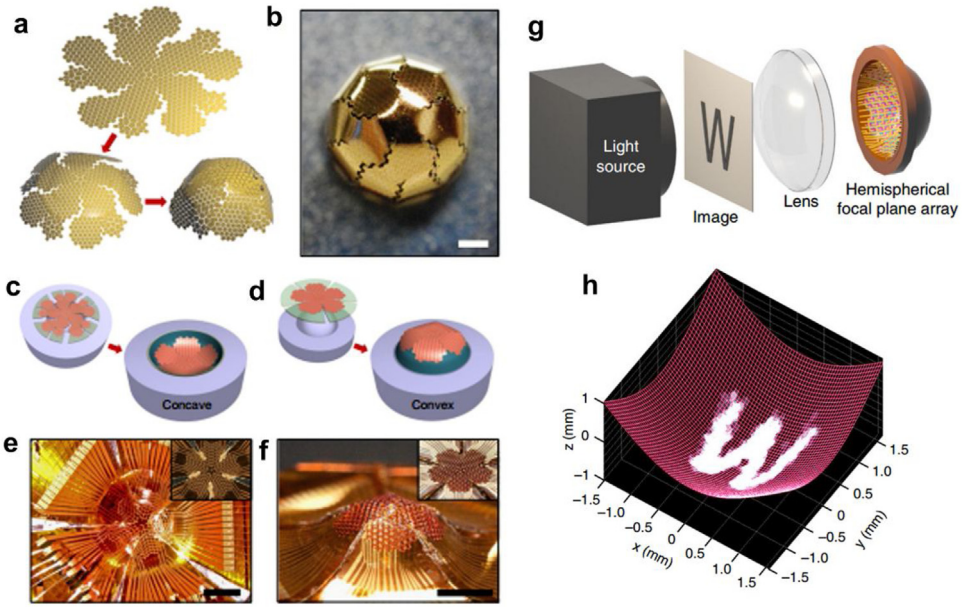


**Fig. 10.** (a) Schematic illustration of the process to fold into a hemisphere of the net of half truncated icosahedron. (b) Optical image of the polygonal blocks of metal-coated silicon nanofilms on flexible polyimide films. (c–d) Schematic illustration of the half truncated icosahedron pressed into a hemispherical concave mold and covered on a hemispherical convex mold. (e–f) Optical image of hemispherical focal plane array based on silicon optoelectronics used by the concave mold and convex mold-based origami approach (g) Optical device of hemispherical electronic eye system. (h) High-resolution image of the letter 'W' obtained from the hemispherical electronic eye camera. Reproduced with permission [19]. Copyright 2017 Nature Publishing Group.

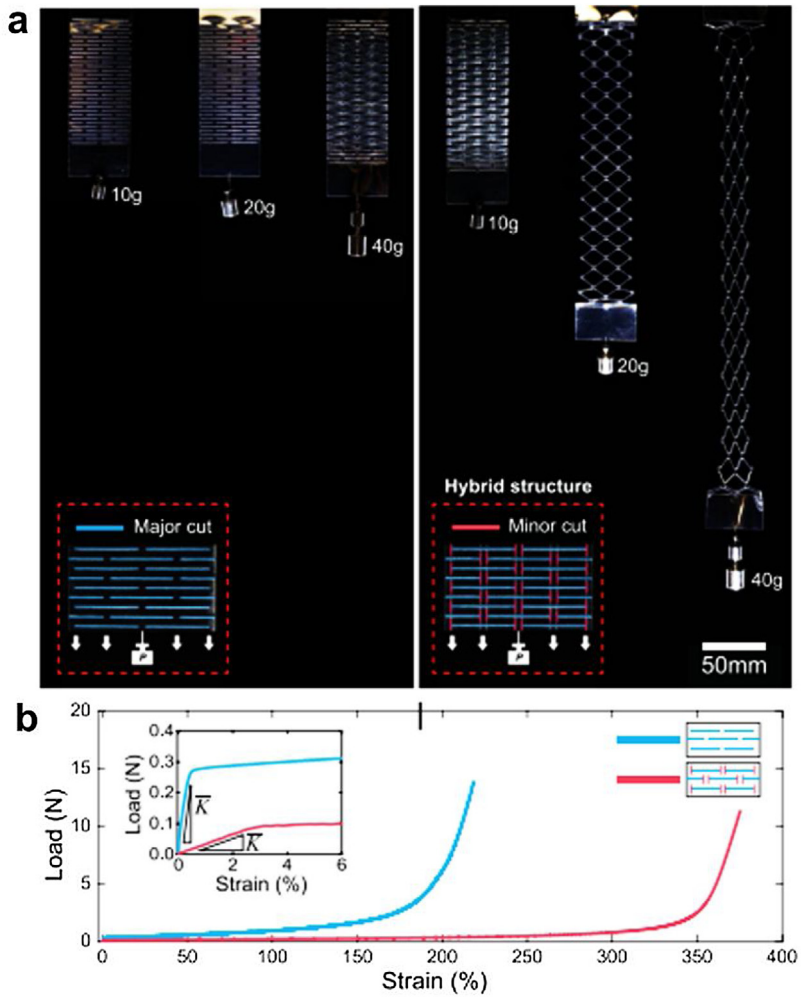


**Fig. 11.** (a) Photographs of kirigami sheets with major cuts (left) and major and minor cuts (right) under external force (10 g, 20 g, and 40 g) (b) Mechanical response of kirigami sheets with different cuts. Reproduced with permission [57]. Copyright 2018 Nature Publishing Group.

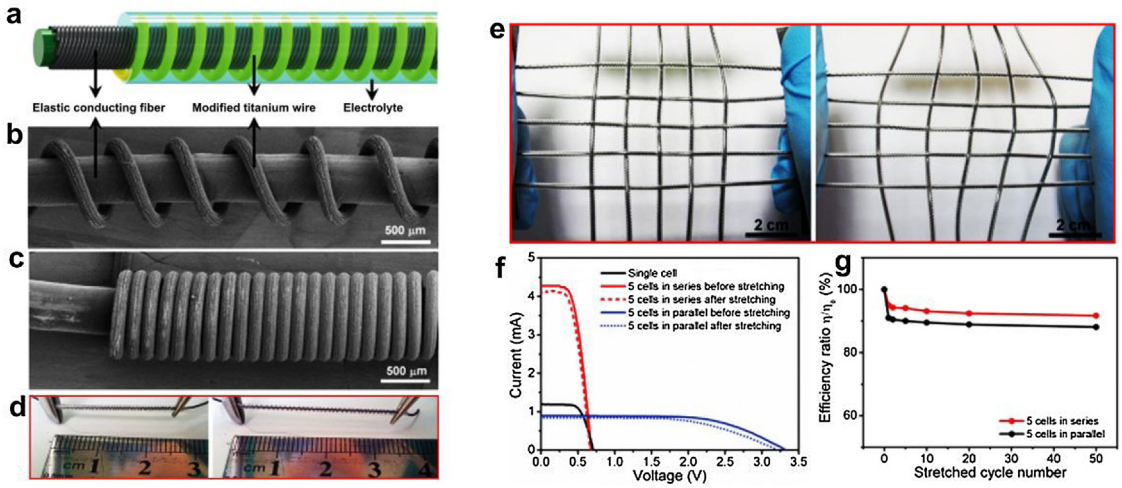


**Fig. 12.** (a) Schematic illustration of a stretchable dye-sensitized solar cell. (b–c) SEM images of stretchable dye-sensitized solar cells with spacing of 560 and 164 μm, respectively. (d) The device before and after stretch by 30%. (e) Optical images of a photovoltaic textile before and after stretch, respectively. (f) J—V curves of the photovoltaic textile in series and parallel before and after stretching. d) Dependence of energy conversion efficiency on tensile Cycle number at strain of ~20%. Reproduced with permission [92]. Copyright 2014 WILEY-VCH Verlag GmbH & Co. KGaA.

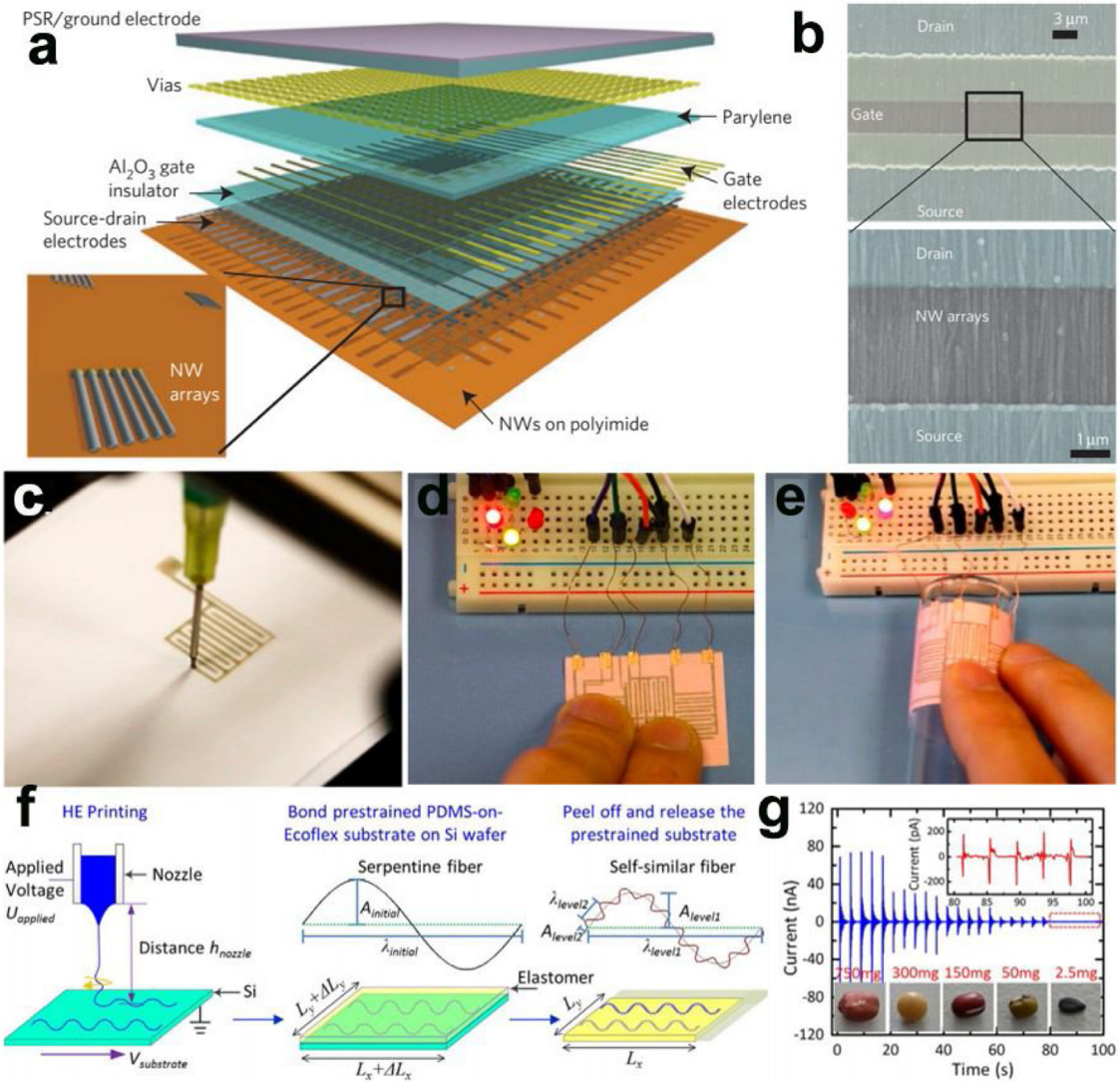


**Fig. 13.** (a) Schematic of the passive and active layers of NW array pressure sensors. (2) SEM images of a NW-array field effect transistor. Reproduced with permission [102]. Copyright 2010, Nature Publishing Group. (c) Images of silver nanowire ink writing on a touchpad. (d) Two fingers touched on the unfolded touch pad and (e) on a curved surface. Reproduced with permission [109]. Copyright 2014, ACS Publications (f) Schematic diagram of fabrication processes of self-similar nano/microfibers. (g) Sensing of different grains, such as sesame, mung bean, azuki bean, soybean, peanut. Reproduced with permission [110]. Copyright 2017, Elsevier Ltd.

Capacitance sensors measure different external pressures or shears by monitoring capacitance changes [111]. Lee et al. proposed to use advanced 3D technology to manufacture biocompatible wireless pressure sensors and biodegradable intelligent polymer scaffolds [112]. Then, the as-prepared wireless pressure sensor is integrated into the polymer scaffold to form an intelligent scaffold platform, which has wireless pressure sensor and can monitor the blood pressure in real time. The unique design of smart stents could minimize periodic medical examinations and control drug doses after stent implantation. Other programmable technologies, such as direct writing, have also been used to fabricate high-performance capacitive pressure sensors. Hu et al. first described the process of writing directly on paper using silver NW ink through a programmable 2D platform (as shown in Fig. 13c–e) [109]. The thickness and electrical properties of the silver NWs directly deposited before and after in situ sintering were studied using different geometric shapes on the touch panel and compared with detailed theoretical designs and the results of experimental analyses. Direct writing technology has the advantages of allowing a low cost and rapid sintering and producing one-time use devices that are ultrathin, ultralight, and have large mechanical flexibility.

Other sensors are based on piezoelectric sensing. The presence of an electric dipole moment generates an electric charge in some materials under mechanical force [113]. In recent years, HE printing technology has been proposed to realize the controlled direct writing of snake-shaped micro/nanofibers with a large area and high level of orientation by introducing the rope effect in the printing process, which has shown a strong capability for the multipurpose and rapid manufacturing of flexible/scalable electronic devices [46]. For example, Yin et al. introduced a new HE printing technology to fabricate snake-like/self-similar fiber structures from piezoelectric polymer materials in a low-cost, large-scale and aligned manner (Fig. 13f) [110]. The superstretchable self-powered sensor adopts a s̈elf-similard̈esign and provides a unique s̈pring-on-springs̈tructure to enhance the tensile properties, i.e., the prestress is greater than the initial stress on the serpentine nano/microfibers. The optimized device showed excellent performance, with a low detection limit of 0.2 mg as shown in Fig. 13g. The design, manufacture and application of HSS were also studied experimentally and theoretically in this study. In summary, research shows that HE printing technology can be used to construct a variety of sensory components, with good mechanical properties at a large scale and low cost, which have the potential for application in devices for human gesture recognition, motion monitoring and other wearable electronic products.

*Strain sensors*

A strain gauge or strain sensor is a sensor used to measure the deformation of an object [114]. Normally, strain gauges consist of patterned metal foils on flexible substrates, which can be easily attached to objects to monitor their deformation. Strain sensors are keys to obtaining mechanical feedback from soft mechanical interfaces in soft robots, rehabilitation monitoring, human-computer interactions and medical treatments [115–117]. There are two main types of mechanical forces interacting with tensile strain sensors: in-plane and out-of-plane forces, which can detect the direct tension and out-of-plane interaction of sensors, respectively [118]. Compared with 1D wire-shaped and 2D flat-film strain sensors, 3D structural strain sensors based on new composite materials and MEMS technology have better out-of-plane force sensing performance. For instance, Baur et al. introduced a 3D ḧair-plugärtificial hair sensor (AHS) with high sensitivity, which can be used to detect low-speed airflow omnidirectionally [119]. The sensor is highly durable and can withstand angular deflection of more than 45 angles in any direction without sustaining damage. Simple integration, durability, low power consumption (<10 μW), small size (150–350 μm), and ease of manufacture mark a new paradigm for the design and application of small-scale AHSs. Similarly, Liu et al. developed an AHC sensor inspired by biological hair cells [120]. The detection limit of the device under AC flow in water was less than 1 mm/s. However, the design of 3D stretchable strain sensors with optimized structures is very important for strain direction identification, high stretchability and improved sensitivity for out-of-plane force detection. Recently, Chen et al. reported a 3D architecture stretch strain sensor using 3D printing bonded out-of-plane capillary force-assisted self-pinning CNTs to monitor out-of-plane forces (Fig. 14a) [118]. The 3D stretchable strain sensor worked well under 120% tension strain applied to the sensing unit (Fig. 14b). It can also detect multiple strains and corresponding strain directions using a single sensor with good stability and repeatability (more than 10,000 strain cycles), which is essential for many applications. The mechanism behind this capability can be explained as destroying the symmetry of resistance networks via multiple out-of-plane loops.

Moreover, 3D strain sensors with patterning and matrix shape modification have great advantages. They can absorb strain through micro and macro designs, thus minimizing the damage caused by strain. This is achieved by introducing spring-like deformation into the sensor coating via prestretching and a fractal base shape. Most strains can be used to unlock springs, and only a small strain far below the fracture strain limit of the coating is transferred to the conductive coating. Several research groups have focused on the application of macroscale or microscale technologies, such as kirigami, 3D printing, and etching, in this field [94,123,124]. Rossiter and his group studied a kirigami technique with a linear cutting mode and designed a stretchable piezoelectric strain sensor with unique 3D architectures, leading to high performance in large strain measurements [124]. Muth et al. developed a high elastic strain sensor based on carbon-based resistance ink [121]. The strain sensor was printed in a glove-shaped reservoir, producing a glove that could be worn on the user's hand to monitor finger movements, shown in Fig. 14c–d. Recently, by means of selective activation, pressure is applied between the discharge table and the nozzle tip to break the oxide shell and merge the liquid core, thus forming a conductive path. The results showed that the process could be used to fabricate printed electronic devices with complex geometries. For instance, a coil pressure sensor and a snake-shaped strain sensor with good flexibility and stretchability have been developed (as shown in Fig. 14e). This technology provides a feasible method for manufacturing polymer tactile sensor based on liquid metal.

The bioinspired design of 3D structures is also an effective strategy for fabricating high-performance strain sensors [125]. In fact, in nature, animals and plants, such as spiders, which have unique 3D structures, have evolved flexible sensors to sense the mechanical signals caused by this deformation force [126]. In recent years, inspired by mammalian whiskers, Javey et al. developed 3D electronic whiskers based on the highly tunable composite films of CNTs and silver NPs using elastic fibers with high aspect ratios as templates [122]. The fabrication progress is shown in Fig. 14f. Because of the whisker structure, the sensitivity of the sensor is higher than most previously reported pressure sensors, and the pressure sensitivity is as high as ~8%/Pa (Fig. 14g). More importantly, electronic whisker arrays with different structures have been designed and successfully applied to 2D and 3D wind field mapping. Other 3D biostructures can also be used in high-performance strain sensors [127]. A layered strain sensor based on ZnO particles has realized static pressure detection of 0.015 Pa and a strain gauge factor >$10^4$ by simulating the bristle characteristics. Such excellent performance further demonstrates the potential application of this sensor technology in the human-machine interface and wearable technology. Recently, electronic whisker has also been used to sense a wide variety of stimuli [128,129]. The

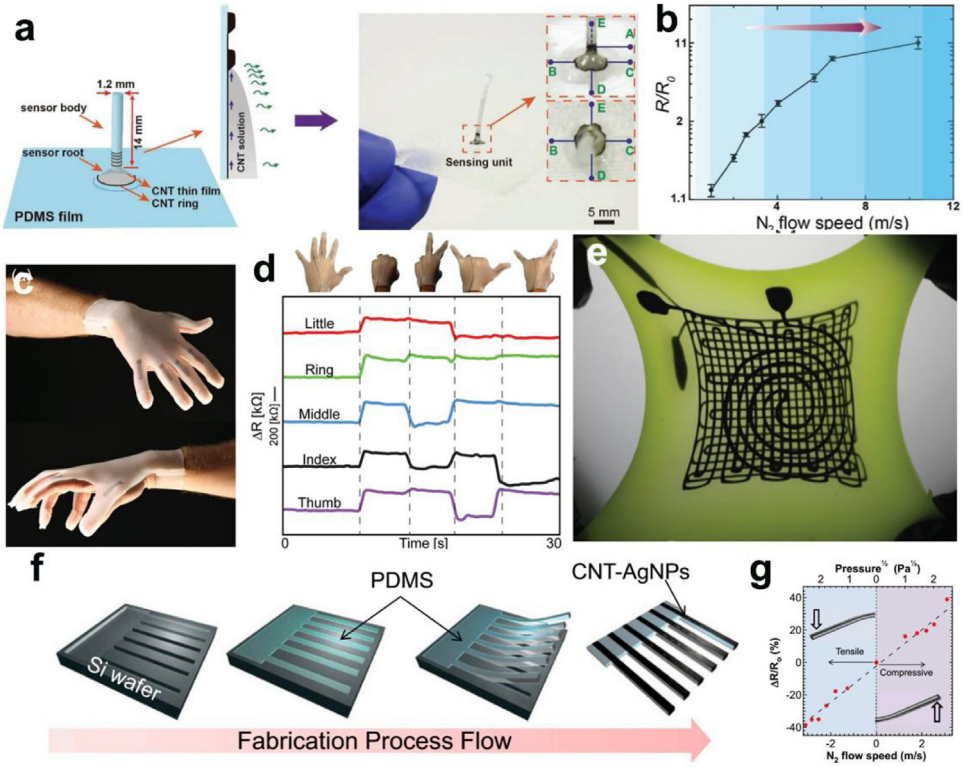


**Fig. 14.** (a) Schematic of the slip-and-stick self-pinning effect (left) and image of the as-fabricated strain sensor with 3D-structured stretchable (right). (b) Resistance response under different speeds. Reproduced with permission [118]. Copyright 2018, WILEY-VCH Verlag GmbH & Co. KGaA. (c) Image of a glove with embedded strain sensors. (d) Electrical resistance change under various gestures within the glove. (e) Optical image of the device in the stretched state. Reproduced with permission [121]. Copyright 2014, WILEY-VCH Verlag GmbH & Co. KGaA. (f) Fabrication process scheme for an e-whisker array. (g) The ΔR/Ro curves induced by gas flow for a representative whisker. Reproduced with permission [122] Copyright 2013, PNAS.

3D assembly of arrays of electronic whisker sensors has been demonstrated by Reeder and his group which can be reconfigured postfabrication [128]. Such arrays of adaptive electronic whiskers can translate proximity, temperature, material stiffness and friction into accurate electrical signals. Furthermore, Takei et al. used the printable nanocomposite inks to fabricate a fully printed multifunctional electronic whisker sensor with good sensing performance to strain and temperature [129]. These two demonstrations exhibit reliable and low-cost methods to develop multifunctional sensors using 3D programmable electronic whisker materials.

*Vibration sensors*

Vibration, a common mechanical movement, is ubiquitous in everyday life, ranging from the operation of household appliances to the bumping of car tires on gravel roads. In recent years, many flexible vibration sensors have been fabricated on ultrathin substrates using micro/nanostructures and piezoelectric materials to sense external vibration stimuli [130,131]. The unique 3D structure of the mammalian basement membrane allows for a high response to certain frequency ranges [134]. These new structural vibration sensors have bioinspired structures to achieve highly efficient and sensitive detection mechanisms. As an example, 3D printing technology has been used to achieve a completely new and feasible way to reproduce the hearing system [132]. This so-called bionic ear is the shape of a human ear printed with hydrogel seeds with living cells; it looks and feels the same as a human ear (Fig. 15a) [132]. Instead of imitating the complex structure of the inner ear and the precise transmission method of mechanoreceptors, the full-functional bionic ear detects sound by receiving electromagnetic signals from a coiled antenna (Fig. 15b). Printed electronic components based on metal NPs form an auditory receiving antenna, and the auricular cartilage printed in vitro shows good structural integrity and shape retention around the coil.

Moreover, complex 3D structures can utilize the advantages of viscoelasticity for the manufacture of highly scalable vibration sensors. Jeong et al. successfully demonstrated the direct printing of elastic conductors, which are embedded on the surface of the elastic substrates instead of printing on or inside, resulting in a highly sensitive vibration sensor [133]. The sensor can detect weak pulses and sound waves, and can be used as recorder, precision pulse detector and printing balance (Fig. 15c-e). Based on the viscoelastic properties of composite materials at high temperatures, a telescopic circuit covering the complex surfaces of 3D objects can be fabricated (Fig. 15f). Very recently, as a potential alternative power source for battery-powered electronic devices, vibration has also become an attractive target for energy collection [135]. Triboelectric nanogenerators (TENG) with unique complex programmable structures could be innovative inventions for collecting environmental mechanical energy as a sustainable power source and activity vibration sensors [135,136]. In recent years, many studies have focused on the reasonably designed 3D structure of TENG that enables TENG to have superior performance in environmental vibration energy acquisition and sensing [137]. First, the new principle of obtaining vibrational energy through TENG based on a harmonic resonator was introduced by Wang et al. [138] In addition, TENG can also be used as a self-powered activity sensor to detect environmental vibrations, such as roadside vibrations triggered by normal human walking. When a person walks to the TENG on the floor naturally, the power output can be obtained successfully. When the maximum effective range is 5 m, the electric output amplitude is exponentially related to the distance between footprint and TENG. Some other 3D advanced materials used in TENG have also been investigated by several groups, which show

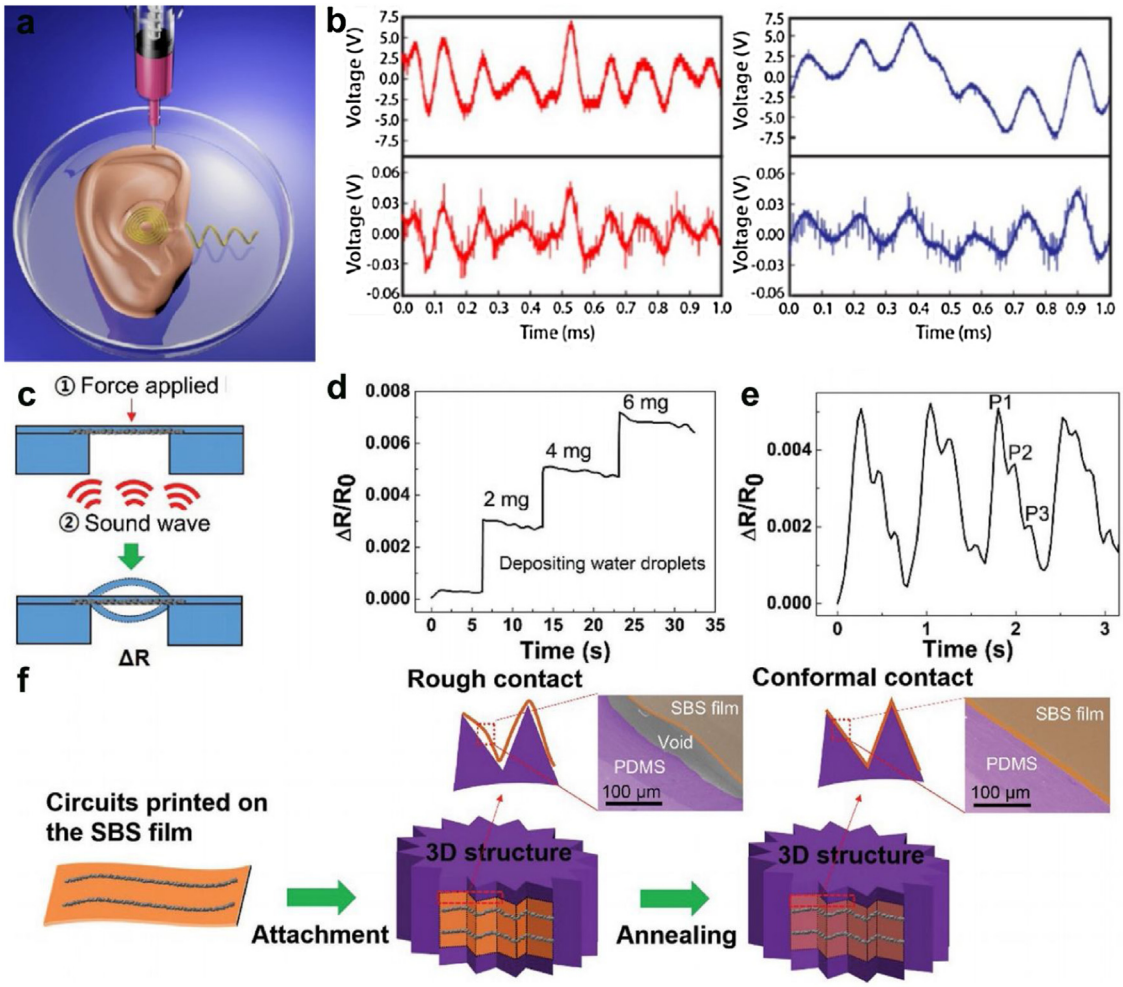


**Fig. 15.** (a) Illustration of the 3D printed bionic ear. (b) Transmitted and received audio signals. Reproduced with permission [132]. Copyright 2013 ACS Publications (c) Schematic illustration of the structure and sensing mechanism. (d) Relative resistance change as depositing the water droplets on the top surface of the sensor. (e) Human pulse measurement from the top surface. (f) Schematic illustration of a stretchable conductive circuit for a 3D structure. Reproduced with permission [133]. Copyright 2017 WILEY-VCH Verlag GmbH & Co. KGaA.

a great self-powered mechanical sensing performance [139–141]. For example, He and his collaborators developed a new type of flexible TENG, which is made by assembling snake-like pattern electrodes and a wavy-structured Kapton film [140]. Due to the unique wavy-structured design, the TENG device can be comfortably attached to human skin to monitor the gentle movement of muscles, joints and even the laryngeal knot. And then similar works have also been introduced by their group. They fabricated the slinky- and doodlebug-shaped TENGs with a short-circuit current of 2 μA and an open-circuit voltage of 20 V using the origami technology by properly folding printer papers [141]. Moreover, the as-fabricated TENGs can obtain environmental mechanical energy from various human movements and used as a self-powered mechanical sensor. These results show that TENG is sensitive to environmental mechanical motions, making it suitable for a variety of energy collection or sensing environments.

*Flexible optical sensors*

The photosensitivity of electronic devices is the primary technology of automobile, biological health monitoring and remote control systems [142–144]. Different device structures, morphologies and materials have been used as phototransistors and photodiodes in photosensitive devices [145–147]. In addition, the high-efficiency and powerful 3D systems, which are regarded as pervasive in biology, show that the same kind of design architecture is likely to be helpful in electronic and optoelectronic devices, by extend their functionality to a level that cannot be achieved using traditional planar 2D platforms. Receiving inspiration from origami and biology, complex 3D structures are anticipated to become a path of 2D-3D conversion. However, current work has yet to achieve the essential mix of functional materials, mechanical design, system-level architecture and the integration capability of practical equipment with unique operating characteristics. This following section provides an introduction of the latest advancements in 3D programmable photosensing technologies.

*Patterning image sensor*

Image sensors are widely used in the national defense, industry, and digital camera fields, among others [148]. Flexible image sensor is an important functional unit of flexible optoelectronic systems. The existing rigid silicon-based image sensor is incompatible with flexible substrate and has low light absorption, which makes it impossible to realize the functions of flexible optoelectronic devices and systems. Fan et al. produced a concept verification image sensor consisting of 1024 photodiode pixels using 3D vertical $MAPbI_3$ NWs [149]. A $10 \times 10$ flexible sensor array with $Zn_2SnO_4$ nanowire photodetectors modified by ZnO quantum dots as sensitive pixels was also studied by our group [150]. It can effectively detect the letters Ëänd Fünder ultraviolet irradiation.

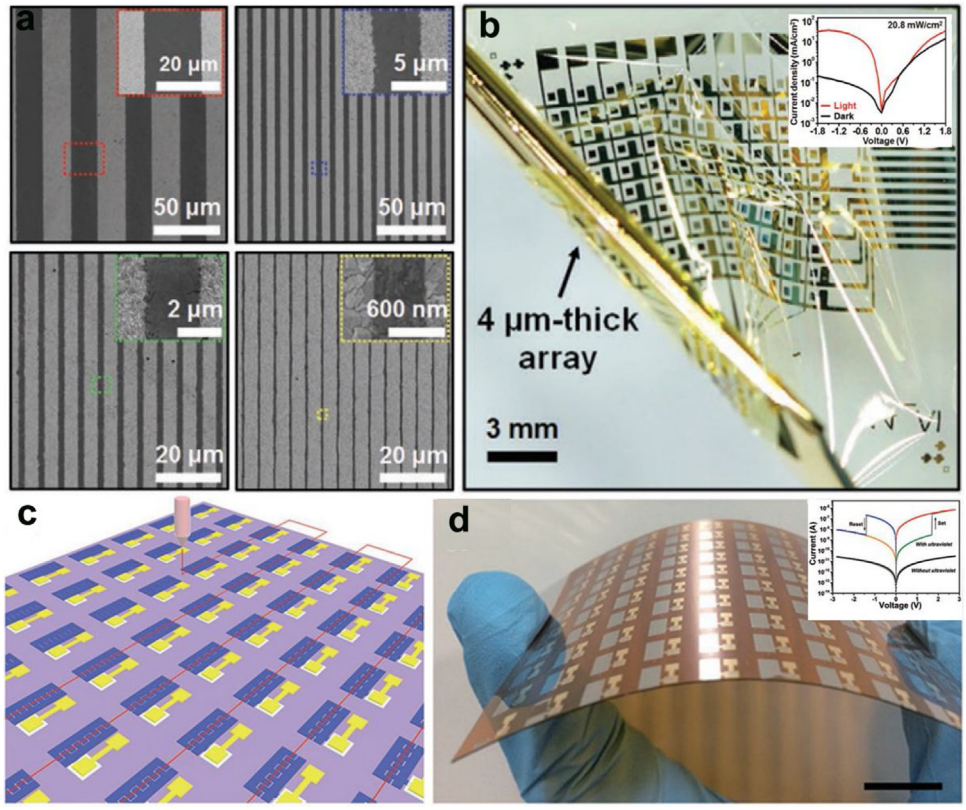


**Fig. 16.** (a) SEM images of different pattern widths of the perovskite films on ITO substrates. (b) Optical image of the ultrathin image sensor array. Inset is the current density–voltage plot. Reproduced with permission [152]. Copyright 2017 WILEY-VCH Verlag GmbH & Co. KGaA. (c) Preparing SMWs on visual memory arrays by the near-field direct-printing process (d) Photograph of the integrated devices arrays on PI substrates. Inset is the typical I–V characteristic of the integrated device without and with UV light illumination. Reproduced with permission [54]. Copyright 2017 WILEY-VCH Verlag GmbH & Co. KGaA.

However, some issues need to be addressed for the fabrication of large-area image sensor arrays. Patterning technology, including inkjet printing, spin-coating and photolithography, is a powerful and cost-effective technology for depositing high-precision, high-resolution photodetectors [151]. It is not only of great significance for graphic applications but also has great potential for photoelectronic direct printing. Kim et al. reported a simple high resolution spin-mode (SOP) process for silicon-based perovskite multi-channel image sensor array. [152]. A high-performance, ultrathin (4 μm) and deformable matrix with a multiplexed patterned perovskite photodiode array was also developed, as shown in Fig. 16a-b. These works provide important guidance for the patterning of perovskite films in multilayered, multiplexed photodiode arrays. However, there are some improvement to be made before large-scale commercialized image sensor applications can be achieved, such as high dark current and low response speed.

Due to the loss of $CH_3NH_3X$ under environmental conditions, the device stability of organic-inorganic hybrid perovskite-based photodetectors is a major concern. In addition to organic-inorganic perovskite, inorganic semiconductors have excellent electronic and photoelectric properties and excellent stability. Recently, our group fabricated high-performance flexible photodetectors on printed aligned $Zn_2GeO_4$ microwire arrays using near-field direct printing [153]. The sensing performance could be adjusted by controlling the patterned microwires. More importantly, we have developed the most advanced image sensors and visual memory systems, which stimulate the logical integration of image sensors and storage devices, thus using the same graphical technology in the bionic design of human visual memory to realize the process of optical information perception and memory, as shown in Fig. 16c–d [54]. By expanding the pixel density of the device array, the optical distribution of patterned images can be detected and written in the visual memory array (10 × 10 pixels). Further improvement of spatial resolution can realize the simulation of capturing and storing high-resolution images in human visual memory. The structure and patterned design of device arrays provide a new way to integrate functional sensors and memory devices, which can be used to simulate human echo memory and tactile memory. Moreover, similar direct printing work on flexible photodetectors has also been reported by several groups [50].

*3D architectures photodetector*

Compared with 2D planar materials, optoelectronic materials deployed in complex 3D structures can provide a relatively high level of functionality. Among recently introduced methods, there is a scheme for the mechanical assembly of fine 3D mesoscopic structures guided by compressive buckling associated with a tensile elastomer matrix [62]. Some designs are reminiscent of those completed on the macroscale via origami/kirigami; these designs have specific shapes and sizes and can span several orders of magnitude in feature size, reach submicron levels in transverse features, and reach tens of nanometers in thickness [21]. Rogers et al. explored the application of 2D $MoS_2$ nanomaterials in functional 3D systems, which were formed by geometric transformation under the guidance of compressive buckling [154]. The structures of the optical sensors with a 3D optical detection/imaging capability are illustrated with as an example. Structures with a 3D light detection/imaging capability were fabricated using a combination of single-layer $MoS_2$ and graphene photosensitive elements; each layer, consisting of $MoS_2$ and graphene, provides an extraordinary combination of optical, mechanical and electrical properties

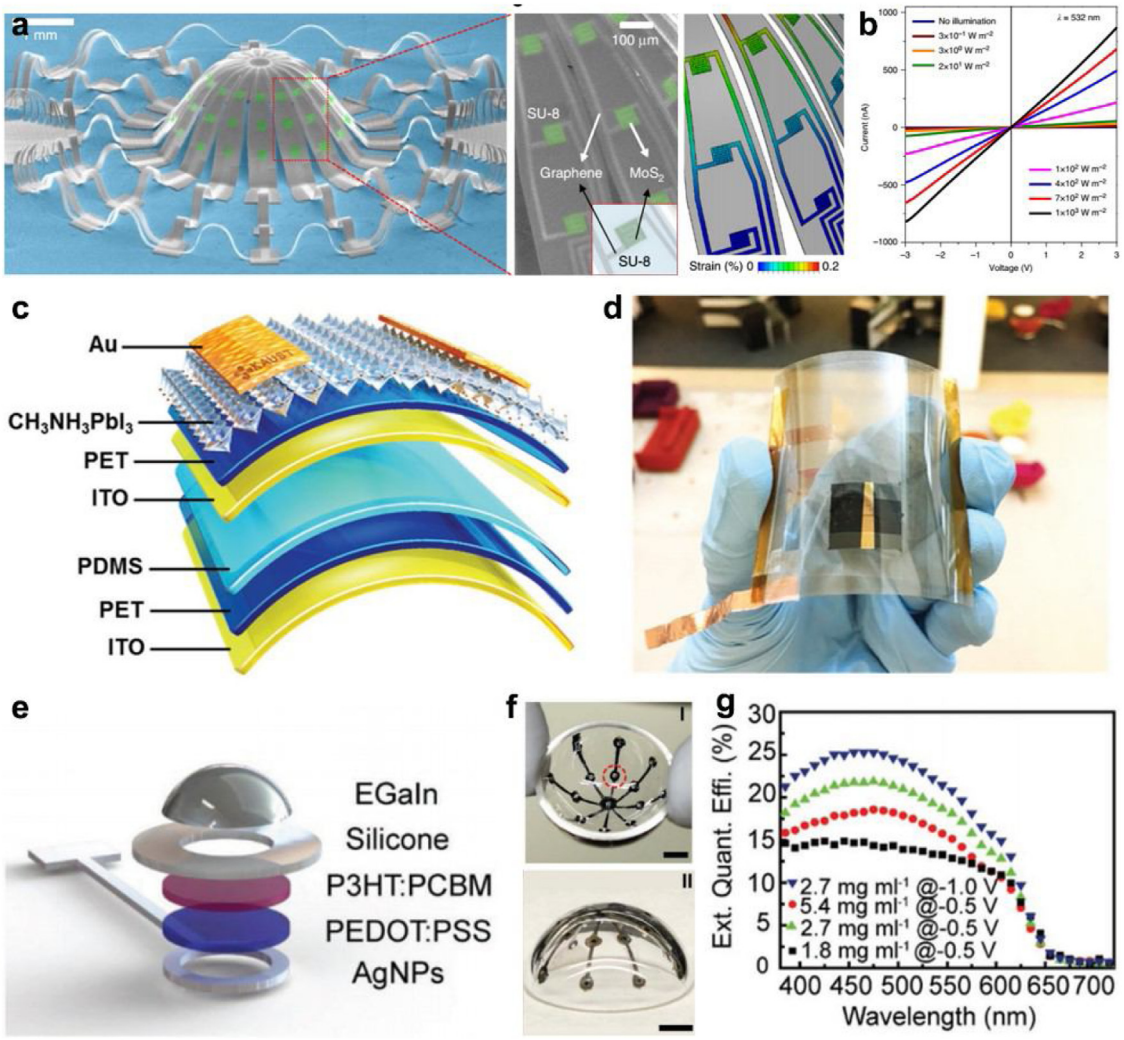


**Fig. 17.** (a) SEM image of the 3D photodetectors consisting of SU-8 (gray), graphene (light gray) and $MoS_2$ (green) on the hemisphere with 3D interconnects. (b) I—V characteristics of the device at different bias voltages under different intensities. Reproduced with permission [154]. Copyright 2018 Nature Publishing Group. (c) Schematic diagram of flexible self-powered photodetector. (d) Optical image of the system. Reproduced with permission [156] Copyright 2018 WILEY-VCH Verlag GmbH & Co. KGaA. (e) Schematic of the structure of the photodetector. (f) Optical images of the concentric photodetector. (g) EQE of the photodetectors with diferent P3HT:PCBM ink concentrations. Reproduced with permission [157]. Copyright 2018 WILEY-VCH Verlag GmbH & Co. KGaA.

related to current applications. Fig. 17a presents a SEM image of the resulting 3D system. Three $MoS_2$ photodetectors have been supported by the hemispherical structure supports on each arm. The entire array consists of 48 devices, all of which are interconnected with a double-layered graphene trace network. The device also shows a good response to visible light (532 nm). Fig. 17b shows the photo response of the device under different illumination intensities. This study may herald other opportunities to design unique system-level functions by deploying 2D materials in 3D design. He et al. demonstrated a low cost and simple paper-based photodetector array that uses printable zinc oxide NWs, carbon electrodes and origami-based technology with excellent deformability [155]. In this study, by combining paper printing, array design and Miura origami, high deformation properties, including torsion (up to 360°), bending (±30°) and tension (up to 1000% strain), can be obtained even when using intrinsically fragile inorganic electronic/optical materials. This origami technology is not only limited to paper-based electronic products, but also can be used in other equipment with hard material characteristics so that they can be stretched or folded. Their group further demonstrates a self-powered flexible photodetector based on the methylammonium lead iodide ($CH_3NH_3PbI_3$) perovskite integrated with the 3D TENG to power this system without external power source as shown in Fig. c–d [156]. This flexible self-powered sensing system shows a large responsivity and an impressive detectivity which can operate under bending and functions at 360 Â° of illumination. Due to these unique features, the flexible 3D self-powered photodetectors can provide a new direction for the next generation of wearable electronics.

The 3D printing of electronic materials is a new method for manufacturing flexible optoelectronic devices [157]. Moreover, 3D printing can realize seamless and multi-functional integration of various devices on a single platform, improving the flexibility of the next generation wearable and 3D photoelectric equipment design and manufacture, and reducing the demand for traditional micro-manufacturing. For example, McAlpine et al. designed a 3D printed polymeric photodetector with high sensing performance, as shown in Fig. 17e-f [157]. A semiconductor polymer ink was printed and optimized for the sensing materials of photodetectors. The external quantum efficiency (EQE) reached 25.3%, which was comparable to that of similar microfabricated products but was produced using only various customized 3D printing tools under environmental conditions (Fig. 17g). The device is integrated into an image sensor array with high response and wide field of view by directly

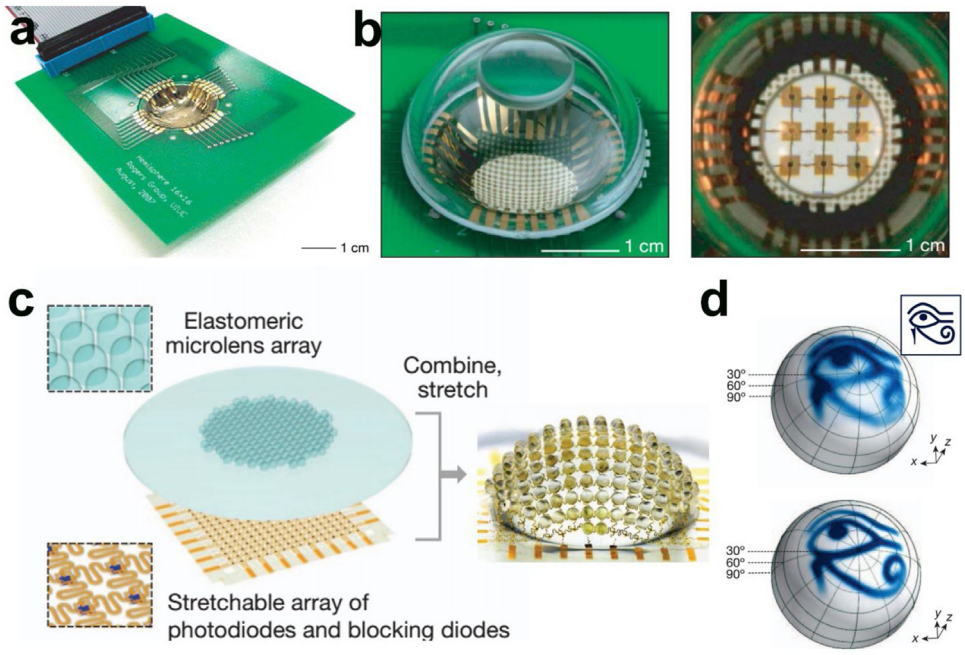


**Fig. 18.** (a) Optical images of a hemispherical focal plane array mounted on a printed circuit board. (b) Optical images of the integrated camera. Reproduced with permission [158]. Copyright 2017 Nature Publishing Group. (c) Illustrations of an array of elastomeric microlenses and supporting posts and image of a representative system after hemispherical deformation. (d) Pictures of line-art illustrations of a 'Horuseye' [163]. Copyright 2013 Nature Publishing Group.

printing interconnected photodetectors on flexible substrates and hemispheres

However, there are also some issues that need to be addressed, including improving the sensing performance and sensing resolution, integrating onboard power options, and implementing adaptive printing on the human body.

*Eye-inspired 3D photodetector array*

Animal eyes have hemispherical photoreceptors for the purpose of the appropriate collection of incoming light. Digital image sensors provide exclusive imaging advantages in the hemispherical geometry, for instance, a broad field of view, coupled with low aberration, compared with their planar counterparts [134]. However, transforming microscale semiconductor-based sensors that have high spatial resolution into this format is quite challenging. Previously, a method of fabricating hemispherical focal plane arrays using semiconductor photodetectors was put forward for the purpose of overcoming this challenge, and transfer printing technology has been applied to deform ultrathin semiconductor films on soft elastomer substrates (Fig. 18a-b) [158]. In addition, in this primary adaptation of the bending image sensor arrays, photodiodes, which are based on silicon nanofilms, was combined with the use of deformable electrical microwires such that the pixels are not impacted by the compression or stretching that occur while they bend onto the hemisphere with the transfer of the whole array to a soft elastomer.

Furthermore, a straightforward origami methodology for the fabrication of monocrystalline silicon-based focal plane arrays and compound eyes with hemispherical structures has been reported [19]. This silicon-based focal plane array houses over 250 photodetectors in a concentrated and compact array. A simple geometric design that could be folded into a sphere was put to use as a predesigned truncated network of decahedrons. Subsequently, the mesh was folded into a hemisphere that perfectly matches the corners of the pixels in the mesh. The results show that a picture captured by means of a spherical, faceted photodetector that does not have a precise optical element. The further development of hemispherical focal plane arrays adds filling factors [159,160]. Choi et al. developed a high-density, hemispherical curved image sensor array, which was designed using atomic-level thin $MoS_2$/graphene heterostructures and strain-release devices [161]. This pioneering bio-inspiration method provides superior imaging capability with simple optical elements. More importantly, it can also achieve unique infrared imaging. Moreover, Jiang et al. described an artificial eye inspired by omental structure and superimposed compound eye [162]. Due to the 3D omnidirectionally aligned optical sensors, the image intensity have a great enhancement without consuming power. Fig. 18c–d shows that a stretchable photodiode and blocking diode array is connected to a snake-shaped interconnection printed on an elastic substrate and then transformed into a convex hemisphere with the use of a hydraulic actuator has also been reported [163]. In addition, the uniform pressure exerted by the hydraulic actuator forms an almost complete hemisphere comprising a number of photodetector pixels, similar to insect eyes. The convex microlens and the supporting column are positioned at the uppermost part of all the pixels, corresponding to a single ommatidium corneal lens and a crystal cone.

*Flexible biological sensor*

With the potential application of wearable biosensors in personal health care and disease diagnosis, wearable biosensors have been widely used to detect various biological indicators, including protein, DNA, organic molecules, cells, and pH [10,164,165]. Flexible biosensors based on 3D structures can rapidly measure input signals with a linear dynamic sensing range and good limit of detection (LOD), along with other significant quantitative analytical performance characteristics. There are many methods for fabricating biosensors based on 3D structures, including the inkjet printing of liquid sensing elements, injection molding after soft lithography, and semiconductor lithography after coating [166–168]. The use of 3D printed biosensors in biosensing has the advantages of high-sensitivity detection, less quantitative analysis, complex batch production and the rapid fabrication of fine structures and

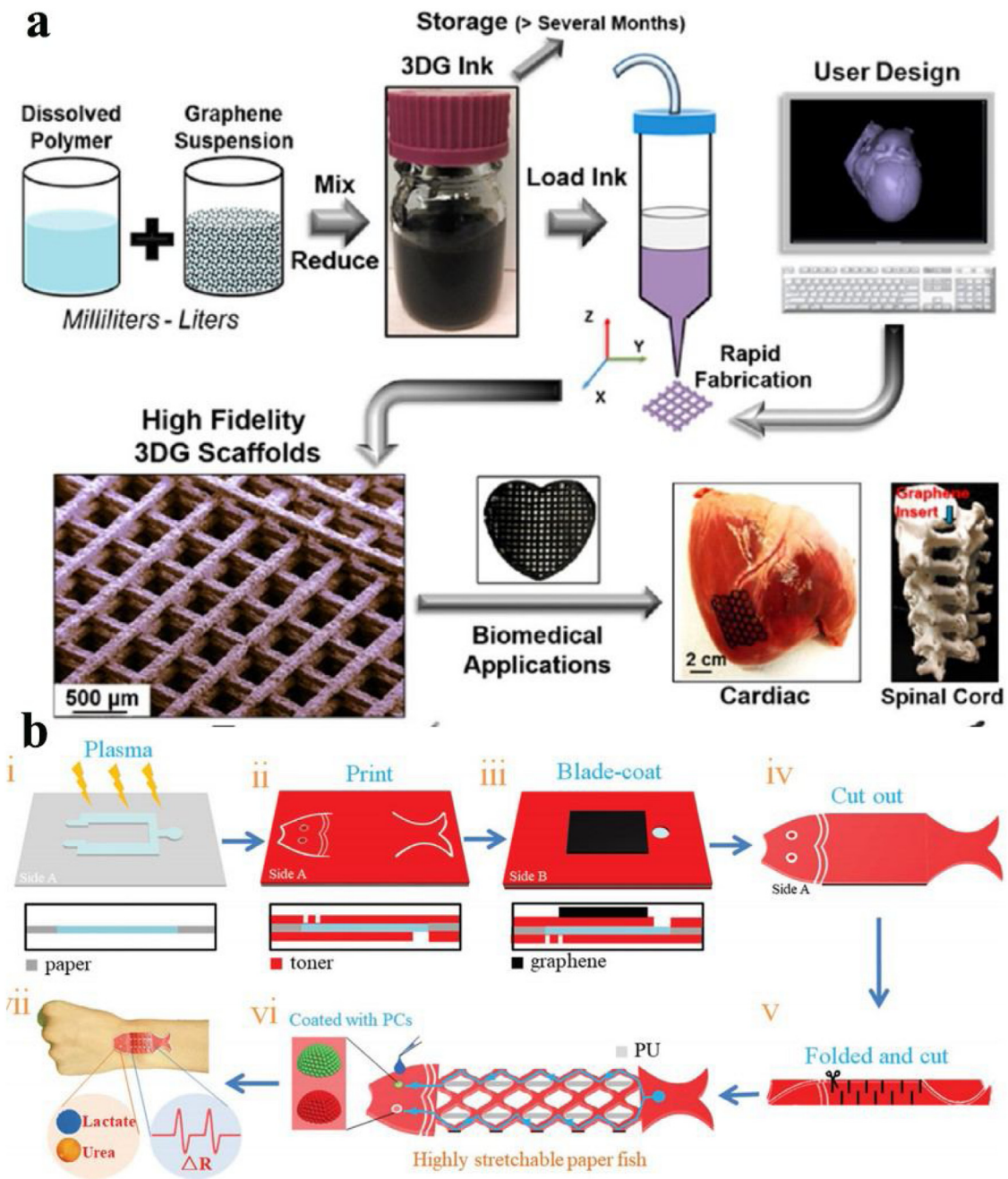


**Fig. 19.** (a) The progress of the user-defined architectures 3D-printed from 3DG. Reproduced with permission [169]. Copyright 2015 ACS Publications. (b) Schematic illustration of the paper fish sensor fabrication process. Reproduced with permission [172]. Copyright 2018 WILEY-VCH Verlag GmbH & Co. KGaA.

functional devices for the assembly of specific biosensors; furthermore, the geometry of devices can be easily changed to make them compatible for use with commercial products. Shah et al. demonstrated the use of a 3D printable graphene (3DG) composite, which consists of mostly graphene and a few polylactic acid copolymers and can be printed in 3D with liquid ink (Fig.19a) [169]. In a vitreous experiment with simple growth medium, without neurogenic stimulation, 3DG supported the adhesion, survival, proliferation and neurogenic differentiation of human mesenchymal stem cells (hMSCs) and significantly upregulated the expression of glial and neurogenic genes. These findings are consistent with the highly slender morphological structure of hMSCs, which is similar to those of axons and presynaptic terminals. In addition, 3D printing technology can be directly used in the manufacturing of biosensors, especially microfluidic devices. A microfluidic device equipped with polyester film and electrodes was prepared by Elkar et al. [170] The microfluidic device could be easily removed for reuse after exposure to flowing erythrocytes. Polyester membranes were used to detect biologically related adenosine triphosphate (ATP) molecules, and electrodes were used to simultaneously determine reduced oxygen concentrations. Wang and his group fabricated a flexible glove-based electrochemical biosensor by the programmable printed electrode system [171]. This programmable glove integrated real-time wireless data transmission device, sampling finger and biosensor detection finger which can address the challenges associated with chemical threat detection and reliable and rapid on-site screening. This study provides a new perspective for the next generation of flexible biosensors.

Biologically stimulated reentrant structures have been proven to be an effective way to achieve high-performance flexible biosen-

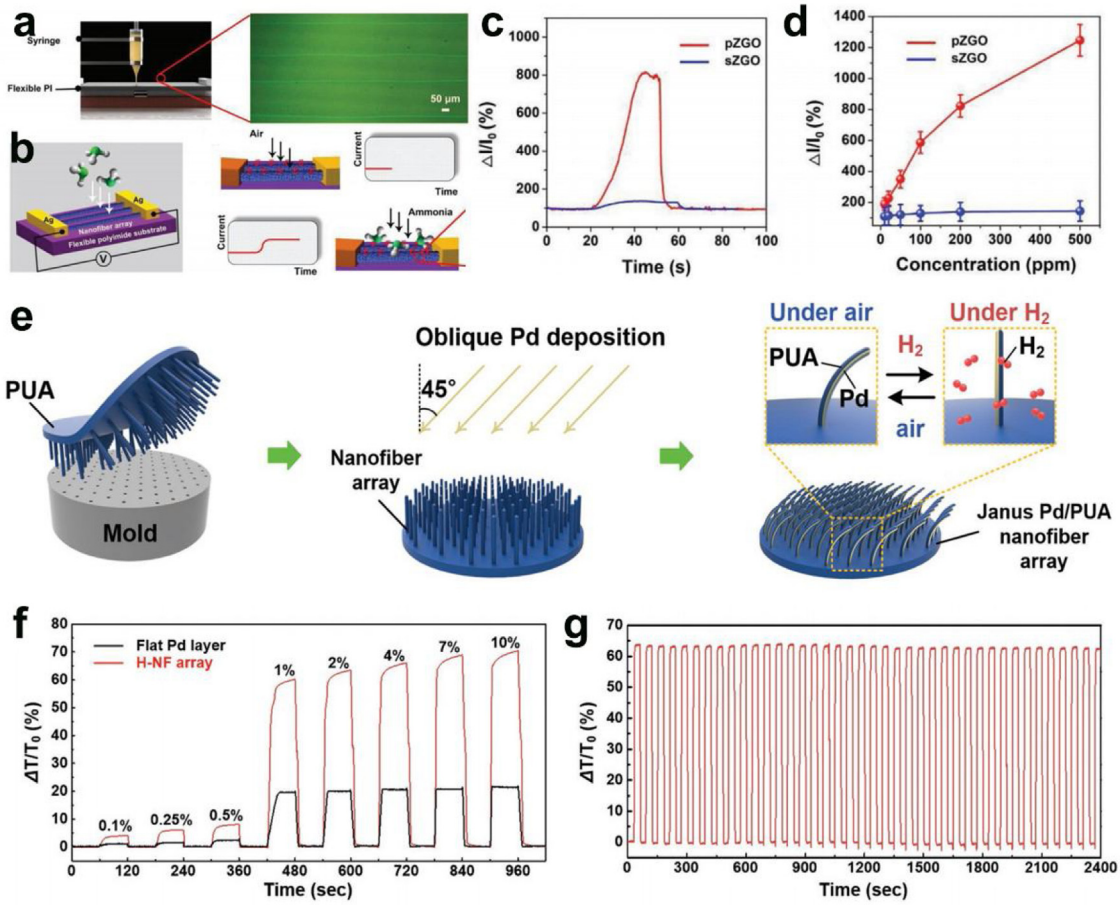


**Fig. 20.** (a) Schematic diagram of printing setup. (b) Schematic of pZGO sensors and the chemical sensing tests. (c) Dynamic sensing response of the pZGO and sZGO for 200 ppm $NH_3$ gas, respectively. (d) Sensitivity plots of sZGO and pZGO devices to 10–500 ppm $NH_3$ gas. Reproduced with permission [49]. Copyright 2019 WILEY-VCH Verlag GmbH & Co. KGaA. (e) Schematic illustration of the H-NF array fabrication procedure. (f) Real-time gas sensing property based on an H-NF array. (g) Repeatability of the device upon loading/unloading 4 vol% $H_2$ in $N_2$. Reproduced with permission [182]. Copyright 2018 WILEY-VCH Verlag GmbH & Co. KGaA.

sors. For example, the liquid surface was studied by 3D printing technology based on two-photon polymerization [173]. The technology also has potential for applications in electronic devices, gas sensors, microchemical/physical reactors, high-throughput biosensors and optical displays. Inspired by fish scale patterns and kirigami art, these researchers also designed and manufactured fish-shaped, wearable biosensors (Fig. 19b) [172]. Paper was coated with conductive graphite paint on one side and then folded via kirigami to obtain stretchable paper substrates. This highly stretched, fully inflated, disposable, wearable fish label enables sweat collection, diagnosis and motion monitoring. The authors also noted that the paper sensor was tunable and that various stretchable patterns with different elongation lengths can be obtained by adjusting the design. This fish-shaped sticker successfully combines the functions of health monitoring and body decoration, and its appearance facilitates the acceptance of children and adolescents. Additionally, inspired by insect tentacles, Zhao and his group developed an antenna-like heterostructure consisting of Prussian blue nanotube and $TiO_2$ nanowire [174]. Such bioinspired structure has an effective 3D interface to sense cell activities and small molecules as biosensors. The as-fabricated biosensors show a great $H_2O_2$ sensing performance with a long-term biocatalytic activity, short response time, and broad detection range due to the forming of biointerfaces. As a proof of bioinspired concept, McLamore et al. also fabricated a low cost and high efficiency biosensor based on 3D patterning of bionanocomposite networks [175]. Similarly, the biomimetic nanostructures can great enhance the sensing performance like hysteresis, LOD, response time and so on. The above studies not only provide the methods for 3D inspired structure but also suggest the uniqueness of the programmable biomimic for biosensing.

*Flexible gas sensor*

With the increasing severity of atmospheric issues, gas sensors capable of monitoring and controlling atmospheric contaminants have attracted the interest of many scholars across the globe [49,176–181]. Grain boundaries offer insistent inspiration, together with potential ways to design state-of-the-art gas sensing nanomaterials [49,176]. In addition, the bulk flaws existing in conjunction with polycrystalline substances have been revealed to produce a wealth of fresh electronic structures, coupled with the catalytic activity and mechanical characteristics involved in a number of applications. Direct writing technology is considered an effective methodology for the fabrication of grain boundary-based gas sensors with a 3D structure. Wang et al. recently performed a study addressing the impacts of bulk defects on polycrystalline-based, printable, flexible gas sensors (Fig. 20a) [49]. In addition, additive defects existing in similar devices are considered the primary parameters impacting not only the electronic but also the catalytic and mechanical characteristics of inorganic semiconductor materials (Fig. 20b). Therefore, it is possible to obtain ultrahigh chemical sensitivity to ammonia (598%, 100 ppm) using printed polycrystalline $Zn_2GeO_4$ wires (pZGO), which is among the greatest sensitivities attained by any kind of ammonia-based chemical sensor (Fig. 20c and d). Furthermore, the pZGO with GBs has an

outstanding mechanical robustness. After repeated folding ($0\tilde{6}0$), the stability of its sensitivity was as high as 831% at RT (room temperature), and the pZGO with GBs device itself lasted for up to 60 days. In the meantime, the initial sensitivity remained more than 88.6%. This advanced manufacturing technology, coupled with the unique device structure, opens up a new avenue for the application of polycrystalline substances in next-generation wearable devices and other applications.

Nanoscale architectures in nature have exclusive functions, and their exploration has resulted in substantial progress in different areas, including adhesion, wetting and optics. As established, the antennae of insects are hypersensitive and respond ultra-rapid to different types of mechanical and chemical signals, because their unique fibrous structure is linked to the mechanical/chemosensory organs [183]. In this manner, Lee et al. proposed a highly sensitive, readable and flexible hydrogen sensor based on $H_2$ reactive Janus nanofibers (H-NFs) stimulated by sensors, in which one side of the polymer nanofibers was coated with a layer of hydrogen sensing metal (Pd) (Fig. 20e) [182]. They made use of and reduced the key structural attributes of the insect sensilla to obtain increased sensitivity, coupled with the quick response time, originating from the exclusive characteristics of the dense array of biased nanofibers. The morphologically controllable H—NF array had high sensitivity, showing a maximum sensitivity of ≈65%, and a quick response time of 5.1 s in response to an existing amount of hydrogen gas (Fig. 20f-g). In addition to the advantages of these outstanding properties, the device also exhibits outstanding mechanical properties, simple chemical functionalization and reasonable in-situ tailoring of natural polysaccharide polymer chemical mixtures. Wang et al. reported a streamlined strategy for simulating the unique surface morphology of natural butterfly wings as multi-functional biomaterial templates, combining the functional properties of graphene [184]. Owing to the small detection constraint of 20 ppb and the ultrafast response time of 1 s, a proof-of-concept wristband embedded into the as-synthesized substance was applied for the purpose of monitoring diabetes-linked acetone fumes in real time. Furthermore, the humidity had a negligible impact on the acetone sensing efficiency, which is highly beneficial for the detection of acetone in respired breath.

## Conclusions and perspectives

3D programmable structures possess all the unique properties of nanomaterials, such as excellent mechanical properties, large surface area, high deformability, excellent transport properties, high-aspect-ratio features, and photoabsorption. Highly ordered and multilevel 3D structures make these materials more suitable as active materials for future flexible sensors. Recent advances have established a series of technologies with astonishing capabilities in the formation of 3D structures, in which key feature sizes can be as small as tens of nanometers, and the thickness and overall spatial range can reach centimeters or more. Various flexible electronic devices, such as flexible mechanical sensors, flexible optical sensors, flexible biological sensors, and flexible gas sensors, have been fabricated using such 3D programmable structure materials. The high performance of these 3D programmable structure materials proves their excellent potential for application in flexible sensors. The capability of fabricating various devices with identical performance on complex 3D structures provides the possibility of constructing high-performance devices with high sensitivity, high resolution and mechanical stability. Despite the 3D programmable structure has achieved great success in manufacturing and application, there are still some problems about advanced materials to be studied in the future. 1) The functionalization and diversity of nanomaterials must be further broad to include the main functional materials integrated with flexible devices. These improvements will certainly provide new functions that ordinary 3D structures cannot provide. 2) The demand for application-related technologies can benefit from 3D geometry, or can be realized through 3D geometry, which will continue to be a powerful driving force for further research in this field. 3) Regardless of the rich patterns/nanostructures which obtained by simple methods, such as printing, folding and lithography, fabricating arbitrary patterns/nanostructure-based flexible sensors remains challenging because of the intrinsic limitations of the size and shape of patterns/structures. Therefore, researchers should combine simple methods to explore more innovative and complete structure. 4) It is very ideal to study the role of 3D programmable nanostructures in the practical application of flexible and wearable sensors and to identify areas for further improvement. With all the features reviewed and promising properties of advanced materials, we expect 3D programmable structures to exhibit new capabilities in applications related to flexible electronics.

## Acknowledgements

Z.L. and L.L.W. contributed equally to this work. This work was supported by the National Natural Science Foundation of China (NSFC, Grant No. 61874111, 61625404, 61888102), Young Elite Scientists Sponsorship Program by CAST (2018QNRC001) and the Key Research Program of Frontier Sciences, CAS (QYZDY-SSW-JWC004).

## References

[1] Z. Lou, L. Li, L.L. Wang, G.Z. Shen, Small 13 (2017) 27.
[2] L.L. Wang, D. Chen, K. Jiang, G.Z. Shen, Chem. Soc. Rev. 46 (2017) 6764–6815.
[3] S.-T. Han, H. Peng, Q. Sun, S. Venkatesh, K.-S. Chung, S.C. Lau, Y. Zhou, V.A.L. Roy,Adv. Mater. 29 (2017), 1700375.
[4] M. Segev-Bar, H. Haick, ACS Nano 7 (2013) 8366–8378.
[5] H. Lee, T.K. Choi, Y.B. Lee, H.R. Cho, R. Ghaffari, L. Wang, H.J. Choi, T.D. Chung, N. Lu, T. Hyeon, S.H. Choi, D.-H. Kim, Nat. Nanotechnol. 11 (2016) 566.
[6] S. Gupta, W.T. Navaraj, L. Lorenzelli, R. Dahiya, NPJ Flex. Electron. 2 (2018) 8.
[7] C.-P. Lee, K.-Y. Lai, C.-A. Lin, C.-T. Li, K.-C. Ho, C.-I. Wu, S.-P. Lau, J.-H. He, Nano Energy 36 (2017) 260–267.
[8] M. Schaffner, J.A. Faber, L. Pianegonda, P.A. Rühs, F. Coulter, A.R. Studart, Nat. Commun. 9 (2018) 878.
[9] Y. Kim, H. Yuk, R. Zhao, S.A. Chester, X. Zhao, Nature 558 (2018) 274–279.
[10] L.L. Wang, J.A. Jackman, W.B. Ng, N.J. Cho, Adv. Funct. Mater. 26 (2016) 8623–8630.
[11] L.L. Wang, W.B. Ng, J.A. Jackman, N.J. Cho, Adv. Funct. Mater. 26 (2016) 2097–2103.
[12] L.L. Wang, K. Wang, Z. Lou, K. Jiang, G.Z. Shen,Adv. Funct. Mater. 28 (2018), 1804510.
[13] M. Han, H. Wang, Y. Yang, C. Liang, W. Bai, Z. Yan, H. Li, Y. Xue, X. Wang, B. Akar, H. Zhao, H. Luan, J. Lim, I. Kandela, G.A. Ameer, Y. Zhang, Y. Huang, J.A. Rogers, Nat. Electron. 2 (2019) 26–35.
[14] K. Bertoldi, V. Vitelli, J. Christensen, M. van Hecke, Nat. Rev. Mater. 2 (2017) 17066.
[15] J. Sha, Y. Li, R. Villegas Salvatierra, T. Wang, P. Dong, Y. Ji, S.-K. Lee, C. Zhang, J. Zhang, R.H. Smith, P.M. Ajayan, J. Lou, N. Zhao, J.M. Tour, ACS Nano 11 (2017) 6860–6867.
[16] S.B. Walker, J.A. Lewis, J. Am. Chem. Soc. 134 (2012) 1419–1421.
[17] Y. Tang, G. Lin, S. Yang, Y.K. Yi, R.D. Kamien, J. Yin,Adv. Mater. 29 (2017), 1604262.
[18] C. Wang, C. Wang, Z. Huang, S. Xu,Adv. Mater. 30 (2018), 1801368.
[19] K. Zhang, Y.H. Jung, S. Mikael, J.H. Seo, M. Kim, H.Y. Mi, H. Zhou, Z.Y. Xia, W.D. Zhou, S.Q. Gong, Z.Q. Ma, Nat. Commun. 8 (2017) 1782.
[20] T.C. Shyu, P.F. Damasceno, P.M. Dodd, A. Lamoureux, L. Xu, M. Shlian, M. Shtein, S.C. Glotzer, N.A. Kotov, Nat. Mater. 14 (2015) 785.
[21] Y. Zhang, Z. Yan, K. Nan, D. Xiao, Y. Liu, H. Luan, H. Fu, X. Wang, Q. Yang, J. Wang, W. Ren, H. Si, F. Liu, L. Yang, H. Li, J. Wang, X. Guo, H. Luo, L. Wang, Y. Huang, J.A. Rogers, Proc. Natl. Acad. Sci. U. S. A. 112 (2015) 11757–11764.
[22] F. Zhang, M. Wei, V.V. Viswanathan, B. Swart, Y. Shao, G. Wu, C. Zhou, Nano Energy 40 (2017) 418–431.
[23] X. Wang, X. Guo, J. Ye, N. Zheng, P. Kohli, D. Choi, Y. Zhang, Z. Xie, Q. Zhang, H. Luan, K. Nan, B.H. Kim, Y. Xu, X. Shan, W. Bai, R. Sun, Z. Wang, H. Jang, F. Zhang, Y. Ma, Z. Xu, X. Feng, T. Xie, Y. Huang, Y. Zhang, J.A. Rogers,Adv. Mater. 31 (2019), 1805615.
[24] D. Rus, M.T. Tolley, Nat. Rev. Mater. 3 (2018) 101–112.
[25] L. Huang, P.-C. Chen, M. Liu, X. Fu, P. Gordiichuk, Y. Yu, C. Wolverton, Y. Kang, C.A. Mirkin, Proc. Natl. Acad. Sci. U. S. A. 115 (2018) 3764–3769.
[26] H. Jiang, P.S. Lee, C. Li, Energy Environ. Sci. 6 (2013) 41–53.

[27] B.L. Ellis, K. Philippe, D. Thierry, Adv. Mater. 45 (2014) 3368–3397.
[28] C.M. Ho, S.H. Ng, K.H. Li, Y.J. Yoon, Lab Chip 15 (2015) 3627.
[29] C. Liu, N. Huang, F. Xu, J. Tong, Z. Chen, X. Gui, Y. Fu, C. Lao, Polymers 10 (2018) 629.
[30] D. Li, W.-Y. Lai, Y.-Z. Zhang, W. Huang,Adv. Mater. 30 (2018), 1704738.
[31] S. Tong, J. Sun, J. Yang, ACS Appl. Mater. Interfaces 10 (2018) 25902–25924.
[32] J.A. Lewis, G.M. Gratson, Mater. Today 7 (2004) 32–39.
[33] B. Derby, Science 338 (2012) 921–926.
[34] Y. Zhang, F. Zhang, Z. Yan, Q. Ma, X. Li, Y. Huang, J.A. Rogers, Nat. Rev. Mater. 2 (2017) 17019.
[35] D. Zhang, B. Chi, B. Li, Z. Gao, Y. Du, J. Guo, J. Wei, Synth. Met. 217 (2016) 79–86.
[36] Y. Lin, Y. Gao, Z. Fan,Adv. Mater. 29 (2017), 1701736.
[37] F. Wang, P. Mao, H. He, Sci. Rep. 6 (2016) 21398.
[38] Q. Li, J.A. Lewis, Adv. Mater. 15 (2003) 1639–1643.
[39] A.S. Sergeev, A.R. Tameev, V.I. Zolotarevskii, A.V. Vannikov, Inorg. Mater. Appl. Res. 9 (2018) 147–150.
[40] V. Francis, P.K. Jain, Virtual Phys. Prototyp. 12 (2017) 107–115.
[41] J. Park, J. Moon, H. Shin, D. Wang, M. Park, J. Colloid Interf. Sci. 298 (2006) 713–719.
[42] E. Sowade, T. Blaudeck, R.R. Baumann, Nanoscale Res. Lett. 10 (2015) 362.
[43] J.E. Smay, G.M. Gratson, R.F. Shepherd, J. Cesarano III, J.A. Lewis, Adv. Mater. 14 (2002) 1279–1283.
[44] G.C. Pidcock, M. in het Panhuis, Extrusion printing conducting gel-carbon nanotube structures upon flexible substrates, (2010).
[45] P.H. Lau, K. Takei, C. Wang, Y. Ju, J. Kim, Z. Yu, T. Takahashi, G. Cho, A. Javey, Nano Lett. 13 (2013) 3864–3869.
[46] D. Ye, Y. Ding, Y. Duan, J. Su, Z. Yin, Y.A. Huang,Small 14 (2018), 1703521.
[47] Z. Liu, L. Jiao, Y. Yao, X. Xian, J. Zhang, Adv. Mater. 22 (2010) 2285–2310.
[48] D.J. Finn, M. Lotya, J.N. Coleman, ACS Appl. Mater. Interfaces 7 (2015) 9254–9261.
[49] L. Wang, S. Chen, W. Li, K. Wang, Z. Lou, G. Shen,Adv. Mater. 31 (2019), 1804583.
[50] X. Liu, L. Gu, Q. Zhang, J. Wu, Y. Long, Z. Fan, Nat. Commun. 5 (2014) 4007.
[51] B. Zhang, B. Seong, V. Nguyen, D. Byun, 3D printing of high-resolution PLA-based structures by hybrid electrohydrodynamic and fused deposition modeling techniques, J. Micromech. Microeng. J. Micromech. Microeng. (2016).
[52] Y.K. Fuh, S.Z. Chen, Z.Y. He, Nanoscale Res. Lett. 8 (2013) 97.
[53] X. Wang, F. Sun, Y. Huang, Y. Duan, Z. Yin, Chem. Commun. 51 (2015) 3117–3120.
[54] S. Chen, Z. Lou, D. Chen, G. Shen,Adv. Mater. 30 (2018), 1705400.
[55] Y. Jiang, Z. Xu, T. Huang, Y. Liu, F. Guo, J. Xi, W. Gao, C. Gao,Adv. Funct. Mater. 28 (2018), 1707024.
[56] C. Zhu, T. Liu, F. Qian, T.Y.-J. Han, E.B. Duoss, J.D. Kuntz, C.M. Spadaccini, M.A. Worsley, Y. Li, Nano Lett. 16 (2016) 3448–3456.
[57] D.-G. Hwang, M.D. Bartlett, Sci. Rep. 8 (2018) 3378.
[58] J. Mu, G. Wang, H. Yan, H. Li, X. Wang, E. Gao, C. Hou, A.T.C. Pham, L. Wu, Q. Zhang, Y. Li, Z. Xu, Y. Guo, E. Reichmanis, H. Wang, M. Zhu, Nat. Commun. 9 (2018) 590.
[59] J. Lyu, M.D. Hammig, L. Liu, L. Xu, H. Chi, C. Uher, T. Li, N.A. Kotov,Appl. Phys. Lett. 111 (2017), 161901.
[60] J. Cui, F.R. Poblete, Y. Zhu,Adv. Funct. Mater. 28 (2018), 1802768.
[61] L. Xu, T.C. Shyu, N.A. Kotov, ACS Nano 11 (2017) 7587–7599.
[62] S. Xu, Z. Yan, K.-I. Jang, W. Huang, H. Fu, J. Kim, Z. Wei, M. Flavin, J. McCracken, R. Wang, A. Badea, Y. Liu, D. Xiao, G. Zhou, J. Lee, H.U. Chung, H. Cheng, W. Ren, A. Banks, X. Li, U. Paik, R.G. Nuzzo, Y. Huang, Y. Zhang, J.A. Rogers, Science 347 (2015) 154–159.
[63] K. Saito, S. Nomura, S. Yamamoto, R. Niiyama, Y. Okabe, Proc. Natl. Acad. Sci. U. S. A. 114 (2017) 5624–5628.
[64] R. Ma, C. Wu, Z.L. Wang, V.V. Tsukruk, ACS Nano 12 (2018) 9714–9720.
[65] M.K. Blees, A.W. Barnard, P.A. Rose, S.P. Roberts, K.L. McGill, P.Y. Huang, A.R. Ruyack, J.W. Kevek, B. Kobrin, D.A. Muller, P.L. McEuen, Nature 524 (2015) 204.
[66] S. Tibbits, Archit. Des. 84 (2014) 116–121.
[67] G. Liu, Y. Zhao, G. Wu, J. Lu, Sci. Adv. 4 (2018), eaat0641.
[68] W. Jiangtao, Z. Zeang, K. Xiao, M.H. Craig, F. Daining, H.J. Qi,Multifunct. Mater. 1 (2018), 015002.
[69] J. Mu, C. Hou, H. Wang, Y. Li, Q. Zhang, M. Zhu,Sci. Adv. 1 (2015), e1500533.
[70] Y. Liu, J. Genzer, M.D. Dickey, Prog. Polym. Sci. 52 (2016) 79–106.
[71] Z. Chen, G. Huang, I. Trase, X. Han, Y. Mei,Phys. Rev. Appl. 5 (2016), 017001.
[72] S.H. Kang, M.D. Dickey, MRS Bull. 41 (2016) 93–96.
[73] T. Paik, S.-H. Hong, E.A. Gaulding, H. Caglayan, T.R. Gordon, N. Engheta, C.R. Kagan, C.B. Murray, ACS Nano 8 (2014) 797–806.
[74] S. Myung, A. Solanki, C. Kim, J. Park, K.S. Kim, K.-B. Lee, Adv. Mater. 23 (2011) 2221–2225.
[75] J.-H. Jang, C.K. Ullal, M. Maldovan, T. Gorishnyy, S. Kooi, C. Koh, E.L. Thomas, Adv. Funct. Mater. 17 (2007) 3027–3041.
[76] O.M. Wani, R. Verpaalen, H. Zeng, A. Priimagi, A.P.H.J. Schenning,Adv. Mater. 31 (2019), 1805985.
[77] S.D. Lacey, D.J. Kirsch, Y. Li, J.T. Morgenstern, B.C. Zarket, Y. Yao, J. Dai, L.Q. Garcia, B. Liu, T. Gao, S. Xu, S.R. Raghavan, J.W. Connell, Y. Lin, L. Hu,Adv. Mater. 30 (2018), 1705651.
[78] M. Liu, P.-Y. Chen, R.H. Hurt,Adv. Mater. 30 (2018), 1705080.
[79] K. Sun, T.-S. Wei, B.Y. Ahn, J.Y. Seo, S.J. Dillon, J.A. Lewis, Adv. Mater. 25 (2013) 4539–4543.
[80] S.H. Kim, Y.K. Yeon, J.M. Lee, J.R. Chao, Y.J. Lee, Y.B. Seo, M.T. Sultan, O.J. Lee, J.S. Lee, S.I. Yoon, I.S. Hong, G. Khang, S.J. Lee, J.J. Yoo, C.H. Park, Nat. Commun. 9 (2018) 14.
[81] C. Cao, J.B. Andrews, A. Kumar, A.D. Franklin, ACS Nano 10 (2016) 5221–5229.
[82] B.G. Compton, J.A. Lewis, Adv. Mater. 26 (2014) 5930–5935.
[83] J.P. Lewicki, J.N. Rodriguez, C. Zhu, M.A. Worsley, A.S. Wu, Y. Kanarska, J.D. Horn, E.B. Duoss, J.M. Ortega, W. Elmer, R. Hensleigh, R.A. Fellini, M.J. King, Sci. Rep. 7 (2017) 43401.
[84] A. Sydney Gladman, E.A. Matsumoto, R.G. Nuzzo, L. Mahadevan, J.A. Lewis, Nat. Mater. 15 (2016) 413.
[85] Z. Song, T. Ma, R. Tang, Q. Cheng, X. Wang, D. Krishnaraju, R. Panat, C.K. Chan, H. Yu, H. Jiang, Nat. Commun. 5 (2014) 3140.
[86] R. Schreiber, J. Do, E.-M. Roller, T. Zhang, V.J. Schüller, P.C. Nickels, J. Feldmann, T. Liedl, Nat. Nanotechnol. 9 (2013) 74.
[87] D.G. Hwang, M.D. Bartlett, Sci. Rep. 8 (2018) 8.
[88] O.M. Wani, R. Verpaalen, H. Zeng, A. Priimagi, A.P.H.J. Schenning,Adv. Mater. 31 (2019), 1805985.
[89] H. Cho, S.M. Kim, Y.S. Kang, J. Kim, S. Jang, M. Kim, H. Park, J.W. Bang, S. Seo, K.Y. Suh, Y.E. Sung, M. Choi, Nat. Commun. 6 (2015) 8.
[90] S. Kawata, H.-B. Sun, T. Tanaka, K. Takada, Nature 412 (2001) 697.
[91] D. Shir, E.C. Nelson, Y.C. Chen, A. Brzezinski, H. Liao, P.V. Braun, P. Wiltzius, K.H.A. Bogart, J.A. Rogers, Appl. Phys. Lett. 94 (2009) 3.
[92] Z. Yang, J. Deng, X. Sun, H. Li, H. Peng, Adv. Mater. 26 (2014) 2643–2647.
[93] L.L. Wang, J.A. Jackman, E.L. Tan, J.H. Park, M.G. Potroz, E.T. Hwang, N.J. Cho, Nano Energy 36 (2017) 38–45.
[94] S.-Z. Guo, K. Qiu, F. Meng, S.H. Park, M.C. McAlpine,Adv. Mater. 29 (2017), 1701218.
[95] Z. Lou, S. Chen, L.L. Wang, R.L. Shi, L. Li, K. Jiang, D. Chen, G.Z. Shen, Nano Energy 38 (2017) 28–35.
[96] Z. Lou, S. Chen, L.L. Wang, K. Jiang, G.Z. Shen, Nano Energy 23 (2016) 7–14.
[97] B.W. An, S. Heo, S. Ji, F. Bien, J.-U. Park, Nat. Commun. 9 (2018) 2458.
[98] S. Lee, A. Reuveny, J. Reeder, S. Lee, H. Jin, Q. Liu, T. Yokota, T. Sekitani, T. Isoyama, Y. Abe, Z. Suo, T. Someya, Nat. Nanotechnol. 11 (2016) 472.
[99] M. Liu, X. Pu, C. Jiang, T. Liu, X. Huang, L. Chen, C. Du, J. Sun, W. Hu, Z.L. Wang,Adv. Mater. 29 (2017), 1703700.
[100] J. Li, R. Bao, J. Tao, Y. Peng, C. Pan, J. Mater. Chem. C Mater. Opt. Electron. Devices 6 (2018) 11878–11892.
[101] Z. Lou, L. Li, L. Wang, G. Shen,Small 13 (2017), 1701791.
[102] K. Takei, T. Takahashi, J.C. Ho, H. Ko, A.G. Gillies, P.W. Leu, R.S. Fearing, A. Javey, Nat. Mater. 9 (2010) 821.
[103] S. Zhang, L. Lou, Y.A. Gu, IEEE Electron Device Lett. 38 (2017) 653–656.
[104] C. Yeom, K. Chen, D. Kiriya, Z. Yu, G. Cho, A. Javey, Adv. Mater. 27 (2015) 1561–1566.
[105] K. Chen, W. Gao, S. Emaminejad, D. Kiriya, H. Ota, H.Y.Y. Nyein, K. Takei, A. Javey, Adv. Mater. 28 (2016) 4397–4414.
[106] M. Gao, L. Li, Y. Song, J. Mater. Chem. C 5 (2017) 2971–2993.
[107] J. Lessing, A.C. Glavan, S.B. Walker, C. Keplinger, J.A. Lewis, G.M. Whitesides, Adv. Mater. 26 (2014) 4677–4682.
[108] Y. Wei, S. Chen, F. Li, Y. Lin, Y. Zhang, L. Liu, ACS Appl. Mater. Interfaces 7 (2015) 14182–14191.
[109] R.-Z. Li, A. Hu, T. Zhang, K.D. Oakes, ACS Appl. Mater. Interfaces 6 (2014) 21721–21729.
[110] Y. Huang, Y. Ding, J. Bian, Y. Su, J. Zhou, Y. Duan, Z. Yin, Nano Energy 40 (2017) 432–439.
[111] O. Kwon, J. An, S. Hong, IEEE Sens. J. 18 (2018) 4832–4846.
[112] J. Park, J.-K. Kim, D.-S. Kim, A. Shanmugasundaram, S.A. Park, S. Kang, S.-H. Kim, M.H. Jeong, D.-W. Lee, Sens. Actuators B 280 (2019) 201–209.
[113] M.T. Chorsi, E.J. Curry, H.T. Chorsi, R. Das, J. Baroody, P.K. Purohit, H. Ilies, T.D. Nguyen,Adv. Mater. 31 (2019), 1802084.
[114] H. Liu, Q. Li, S. Zhang, R. Yin, X. Liu, Y. He, K. Dai, C. Shan, J. Guo, C. Liu, C. Shen, X. Wang, N. Wang, Z. Wang, R. Wei, Z. Guo, J. Mater. Chem. C 6 (2018) 12121–12141.
[115] Y. Guo, Z. Guo, M. Zhong, P. Wan, W. Zhang, L. Zhang,Small 14 (2018), 1803018.
[116] D. Rus, M.T. Tolley, Nature 521 (2015) 467.
[117] Z. Lou, L. Wang, G. Shen,Adv. Mater. Technol. 3 (2018), 1800444.
[118] Z. Liu, D. Qi, W.R. Leow, J. Yu, M. Xiloyannnis, L. Cappello, Y. Liu, B. Zhu, Y. Jiang, G. Chen, L. Masia, B. Liedberg, X. Chen,Adv. Mater. 30 (2018), 1707285.
[119] M.R. Maschmann, G.J. Ehlert, B.T. Dickinson, D.M. Phillips, C.W. Ray, G.W. Reich, J.W. Baur, Adv. Mater. 26 (2014) 3230–3234.
[120] N. Chen, C. Tucker, J.M. Engel, Y. Yang, S. Pandya, C. Liu, J. Microelectromech. Syst. 16 (2007) 999–1014.
[121] J.T. Muth, D.M. Vogt, R.L. Truby, Y. Mengüç, D.B. Kolesky, R.J. Wood, J.A. Lewis, Adv. Mater. 26 (2014) 6307–6312.
[122] K. Takei, Z. Yu, M. Zheng, H. Ota, T. Takahashi, A. Javey, Proc. Natl. Acad. Sci. U. S. A. 111 (2014) 1703–1707.
[123] Y.-S. Guan, Z. Zhang, Y. Tang, J. Yin, S. Ren,Adv. Mater. 30 (2018), 1706390.
[124] R. Sun, B. Zhang, L. Yang, W. Zhang, I. Farrow, F. Scarpa, J. Rossiter,Appl. Phys. Lett. 112 (2018), 251904.
[125] X. Shi, H. Wang, X. Xie, Q. Xue, J. Zhang, S. Kang, C. Wang, J. Liang, Y. Chen, ACS Nano (2018).
[126] D. Kang, P.V. Pikhitsa, Y.W. Choi, C. Lee, S.S. Shin, L. Piao, B. Park, K.-Y. Suh, T.-i. Kim, M. Choi, Nature 516 (2014) 222.
[127] B. Yin, X. Liu, H. Gao, T. Fu, J. Yao, Nat. Commun. 9 (2018) 5161.
[128] J.T. Reeder, T. Kang, S. Rains, W. Voit,Adv. Mater. 30 (2018), 1706733.

[129] H. Shingo, H. Wataru, A. Takayuki, A. Seiji, T. Kuniharu, ACS Nano 8 (2014) 3921–3927.
[130] C. Lang, J. Fang, H. Shao, X. Ding, T. Lin, Nat. Commun. 7 (2016) 11108.
[131] B. Zhang, L. Zhang, W. Deng, L. Jin, F. Chun, H. Pan, B. Gu, H. Zhang, Z. Lv, W. Yang, Z.L. Wang, ACS Nano 11 (2017) 7440–7446.
[132] M.S. Mannoor, Z. Jiang, T. James, Y.L. Kong, K.A. Malatesta, W.O. Soboyejo, N. Verma, D.H. Gracias, M.C. McAlpine, Nano Lett. 13 (2013) 2634–2639.
[133] J.H. Song, Y.-T. Kim, S. Cho, W.-J. Song, S. Moon, C.-G. Park, S. Park, J.M. Myoung, U. Jeong,Adv. Mater. 29 (2017), 1702625.
[134] Y.H. Jung, B. Park, J.U. Kim, T.-i. Kim, Adv. Mater. (2019), http://dx.doi.org/10.1002/adma.201803637.
[135] Y. Chen, Y.-C. Wang, Y. Zhang, H. Zou, Z. Lin, G. Zhang, C. Zou, Z.L. Wang,Adv. Energy Mater. 8 (2018), 1802159.
[136] J. Qian, X. Jing, Nano Energy 52 (2018) 78–87.
[137] M. Salauddin, R.M. Toyabur, P. Maharjan, M.S. Rasel, J.W. Kim, H. Cho, J.Y. Park, Nano Energy 51 (2018) 61–72.
[138] J. Chen, G. Zhu, W. Yang, Q. Jing, P. Bai, Y. Yang, T.-C. Hou, Z.L. Wang, Adv. Mater. 25 (2013) 6094–6099.
[139] B. Meng, W. Tang, Z.-h. Too, X. Zhang, M. Han, W. Liu, H. Zhang, Energ. Environ. Sci. 6 (2013) 3235–3240.
[140] P.K. Yang, L. Lin, F. Yi, X. Li, K.C. Pradel, Y. Zi, C.I. Wu, J.H. He, Y. Zhang, Z.L. Wang, Adv. Mater. 27 (2015) 3817–3824.
[141] Y. Po-Kang, L. Zong-Hong, K.C. Pradel, L. Long, L. Xiuhan, W. Xiaonan, H. Jr-Hau, W. Zhong Lin, ACS Nano 9 (2015) 901–907.
[142] Z. Lou, G. Shen,Adv. Sci. 3 (2016), 1500287.
[143] W. Ouyang, T. Feng, X. Fang,Adv. Funct. Mater. 28 (2018), 1707178.
[144] H. Chen, H. Liu, Z. Zhang, K. Hu, X. Fang, Adv. Mater. 28 (2016) 403–433.
[145] C. Xie, F. Yan,Small 13 (2017), 1701822.
[146] F. Teng, K. Hu, W. Ouyang, X. Fang,Adv. Mater. 30 (2018), 1706262.
[147] C.-H. Lin, H.-C. Fu, D.-H. Lien, C.-Y. Hsu, J.-H. He, Nano Energy 51 (2018) 294–299.
[148] W. Wu, X. Wang, X. Han, Z. Yang, G. Gao, Y. Zhang, J. Hu, Y. Tan, A. Pan, C. Pan, Adv. Mater. 31 (3) (2018), http://dx.doi.org/10.1002/adma.201805913.
[149] L. Gu, M.M. Tavakoli, D. Zhang, Q. Zhang, A. Waleed, Y. Xiao, K.-H. Tsui, Y. Lin, L. Liao, J. Wang, Z. Fan, Adv. Mater. 28 (2016) 9713–9721.
[150] L. Li, L. Gu, Z. Lou, Z. Fan, G. Shen, ACS Nano 11 (2017) 4067–4076.
[151] Z. Zhan, J. An, Y. Wei, V.T. Tran, H. Du, Nanoscale 9 (2017) 965–993.
[152] W. Lee, J. Lee, H. Yun, J. Kim, J. Park, C. Choi, D.C. Kim, H. Seo, H. Lee, J.W. Yu, W.B. Lee, D.-H. Kim,Adv. Mater. 29 (2017), 1702902.
[153] S. Chen, Z. Lou, D. Chen, G. Shen,Adv. Mater. Technol. 3 (2018), 1800050.
[154] W. Lee, Y. Liu, Y. Lee, B.K. Sharma, S.M. Shinde, S.D. Kim, K. Nan, Z. Yan, M. Han, Y. Huang, Y. Zhang, J.-H. Ahn, J.A. Rogers, Nat. Commun. 9 (2018) 1417.
[155] C.-H. Lin, D.-S. Tsai, T.-C. Wei, D.-H. Lien, J.-J. Ke, C.-H. Su, J.-Y. Sun, Y.-C. Liao, J.-H. He, ACS Nano 11 (2017) 10230–10235.
[156] S.F. Leung, K.T. Ho, P.K. Kung, V.K.S. Hsiao, H.N. Alshareef, Z.L. Wang, J.H. He,Adv. Mater. 30 (2018), 1704611.
[157] S.H. Park, R. Su, J. Jeong, S.-Z. Guo, K. Qiu, D. Joung, F. Meng, M.C. McAlpine,Adv. Mater. 30 (2018), 1803980.
[158] H.C. Ko, M.P. Stoykovich, J. Song, V. Malyarchuk, W.M. Choi, C.-J. Yu, J.B. Geddes Iii, J. Xiao, S. Wang, Y. Huang, J.A. Rogers, Nature 454 (2008) 748.
[159] S. Gunchul, J. Inhwa, M. Viktor, S. Jizhou, W. Shuodao, K. Heung Cho, H. Yonggang, H. Jeong Sook, J.A. Rogers, Small 6 (2010) 851–856.
[160] J. Inhwa, X. Jianliang, M. Viktor, L. Chaofeng, L. Ming, L. Zhuangjian, Y. Jongseung, H. Yonggang, J.A. Rogers, Proc. Natl. Acad. Sci. U. S. A. 108 (2011) 1788–1793.
[161] C. Choi, M.K. Choi, S. Liu, S.K. Min, O.K. Park, C. Im, J. Kim, X. Qin, G.J. Lee, K.W. Cho, Nat. Commun. 8 (2017) 1664.
[162] H. Liu, Y. Huang, H. Jiang, Proc Natl Acad Sci U. S. A. 113 (2016) 3982–3985.
[163] Y.M. Song, Y. Xie, V. Malyarchuk, J. Xiao, I. Jung, K.-J. Choi, Z. Liu, H. Park, C. Lu, R.-H. Kim, R. Li, K.B. Crozier, Y. Huang, J.A. Rogers, Nature 497 (2013) 95.
[164] Y. Yang, X. Yang, Y. Tan, Q. Yuan, Nano Res. 10 (2017) 1560–1583.
[165] D. Son, J. Lee, S. Qiao, R. Ghaffari, J. Kim, J.E. Lee, C. Song, S.J. Kim, D.J. Lee, S.W. Jun, S. Yang, M. Park, J. Shin, K. Do, M. Lee, K. Kang, C.S. Hwang, N. Lu, T. Hyeon, D.-H. Kim, Nat. Nanotechnol. 9 (2014) 397.
[166] M. Magliulo, M.Y. Mulla, M. Singh, E. Macchia, A. Tiwari, L. Torsi, K. Manoli, J. Mater. Chem. C 3 (2015) 12347–12363.
[167] J. Li, F. Rossignol, J. Macdonald, Lab Chip 15 (2015) 2538–2558.
[168] Y. Ni, R. Ji, K. Long, T. Bu, K. Chen, S. Zhuang, Appl. Spectrosc. Rev. 52 (2017) 623–652.
[169] A.E. Jakus, E.B. Secor, A.L. Rutz, S.W. Jordan, M.C. Hersam, R.N. Shah, ACS Nano 9 (2015) 4636–4648.
[170] J.L. Erkal, A. Selimovic, B.C. Gross, S.Y. Lockwood, E.L. Walton, S. McNamara, R.S. Martin, D.M. Spence, Lab Chip 14 (2014) 2023–2032.
[171] R.K. Mishra, L.J. Hubble, A. Martín, R. Kumar, A. Barfidokht, J. Kim, M.M. Musameh, I.L. Kyratzis, J. Wang, ACS Sens. 2 (2017) 553–561.
[172] B. Gao, A. Elbaz, Z. He, Z. Xie, H. Xu, S. Liu, E. Su, H. Liu, Z. Gu,Adv. Mater. Technol. 3 (2018), 1700308.
[173] G. Williams, M. Hunt, B. Boehm, A. May, M. Taverne, D. Ho, S. Giblin, D. Read, J. Rarity, R. Allenspach, S. Ladak, Nano Res. 11 (2018) 845–854.
[174] B. Kong, T. Jing, Z. Wu, C. Selomulya, H. Wang, W. Jing, Y. Wang, G. Zheng, D. Zhao,NPG Asia Mater. 6 (2014), e117.
[175] E.S. McLamore, M. Convertino, J. Hondred, S. Das, J.C. Claussen, D.C. Vanegas, C. Gomes,Proc. SPIE. Int. Soc. Opt. Eng. 9863 (2016), 986309.
[176] L.L. Wang, R.Q. Chai, Z. Lou, G.Z. Shen, Nano Res. 11 (2018) 1029–1037.
[177] W. Wei, W. Li, L.L. Wang, Sens. Actuators B 263 (2018) 502–507.
[178] L.L. Wang, Z. Lou, J.N. Deng, R. Zhang, T. Zhang, ACS Appl. Mater. Interfaces 7 (2015) 13098–13104.
[179] L.L. Wang, H.M. Dou, Z. Lou, T. Zhang, Nanoscale 5 (2013) 2686–2691.
[180] Z. Lou, L.L. Wang, R. Wang, T. Fei, T. Zhang, Solid-State Electron. 76 (2012) 91–94.
[181] K. Wang, J. Li, W. Li, W. Wei, H. Zhang, L. Wang,Adv. Mater. Technol. 4 (2019), 1800521.
[182] H. Han, S. Baik, B. Xu, J. Seo, S. Lee, S. Shin, J. Lee, J.H. Koo, Y. Mei, C. Pang, T. Lee,Adv. Funct. Mater. 27 (2017), 1701618.
[183] A. Alfadhel, J. Kosel, Adv. Mater. 27 (2015) 7896.
[184] L. Wang, J.A. Jackman, J.H. Park, E.-L. Tan, N.-J. Cho, J. Mater. Chem. B 5 (2017) 4019–4024.

**Zheng Lou** is an Associate professor in the Institute of Semiconductors, Chinese Academy of Sciences. He received his BS degree (2009) and his Ph.D degree (2014) from Jilin University. His current research focuses on flexible electronics based on low dimensional materials, including pressure sensors, electronic-skin, transistors and photo-detectors.

**Lili Wang** is an Associate professor in the College of Electronic Science and Engineering at Jilin University, China. She earned her B. S. degree (2010) in Chemistry and Ph.D degree in Microelectronics and Solid State Electronics from Jilin University in 2014. She successively became a Lecturer at Jilin University in 2014. Her current research interests focus on the flexible and wearable sensor based on biological materials, 2D materials and metal oxide semiconductor.

**Guozhen Shen** received his B. S. degree (1999) in Chemistry from Anhui Normal University and Ph. D degree (2003) in Chemistry from University of Science and technology of China. He joined the Institute of Semiconductors, Chinese Academy of Sciences as a Professor in 2013. His current research focused on flexible electronics and printable electronics, including transistors, photodetectors, sensors and flexible energy storage and conversion devices.